Search for new physics with one Higgs boson in the bbγγ channel with the ATLAS detector

Maxime Fernoux
PhD defense - 30 September 2024

Jury members :
Anne-Catherine Le Bihan
Tristan du Pree
Stephane Jezequel
Cristinel Diaconu

Supervisors :
Arnaud Duperrin
Elisabeth Petit

Outline

Theoretical introduction and Higgs boson physics overview

The ATLAS experiment

Adaptation of a neural network algorithm for flavour tagging at HL-LHC

Search for additional scalar bosons in the $X \to SH \to bb\gamma\gamma$ channel

Theoretical introduction and Higgs boson physics overview

The Standard Model of particle physics

- The Standard Model (SM) describes and classifies the known elementary particles and their interactions. It's a quantum field theory based on the gauge invariance principle

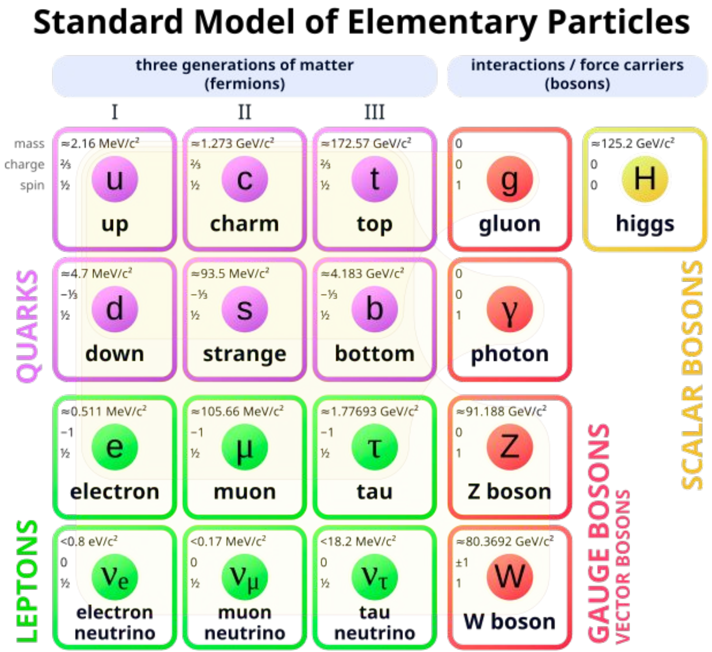

- **Fermions** are the building blocks of matter
They are divided into *quarks* (sensitive to the strong interaction) and *leptons*

- Gauge **bosons** support the interactions between them : the strong, weak and electromagnetic forces

- The **Higgs boson** is notably linked to the mass of the other particles

Higgs mechanism

- The Higgs mechanism explains the mass of the weak interaction bosons by the spontaneous breaking of the gauge symmetry
  → The Higgs field is a scalar field with non-zero vacuum expectation value
  → Other particles acquire their mass by interacting with this field

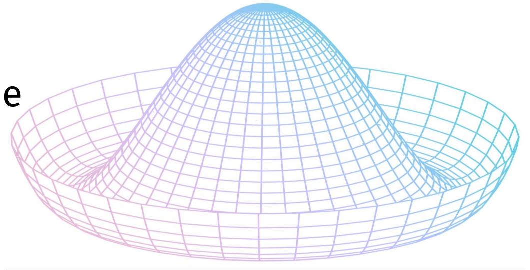

- The Higgs boson is an excitation of this field
  It's a scalar massive particle that was discovered in 2012

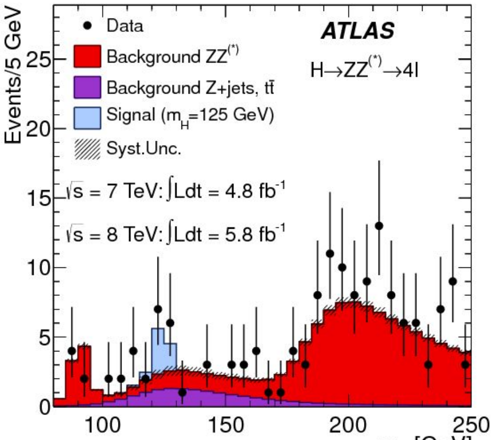

[Phys.Lett. B716 (2012) 1-29]

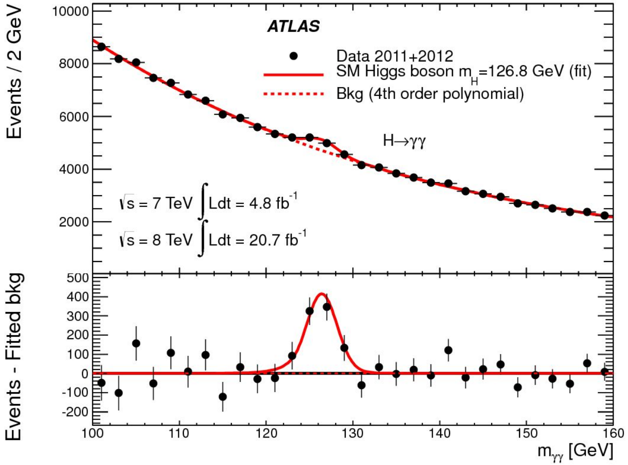

Higgs boson

The Higgs boson has been intensively studied since its discovery

- What we know :
  - Mass : m_{Higgs} = 125.25 ± 0.17 GeV
  - Spin parity = 0^+ - other possibilities excluded at 99% CL
  - Production modes, decay channels
    → Couplings to heavy particles

→ Everything agree with the SM prediction for now

- What remains to discover :
  - Couplings to lighter fermions
  - Higgs self coupling

Decay channel	Branching ratio (%)
$H \to b\bar{b}$	$58.2^{+0.70}_{-0.76}$
$H \to WW^*$	21.4 ± 0.32
$H \to gg$	8.18 ± 0.42
$H \to \tau^+\tau^-$	6.27 ± 0.10
$H \to c\bar{c}$	$2.89^{+0.16}_{-0.06}$
$H \to ZZ^*$	2.62 ± 0.039
$H \to \gamma\gamma$	0.227 ± 0.0048
$H \to Z\gamma$	0.153 ± 0.0089
$H \to \mu^+\mu^-$	0.0218 ± 0.00037

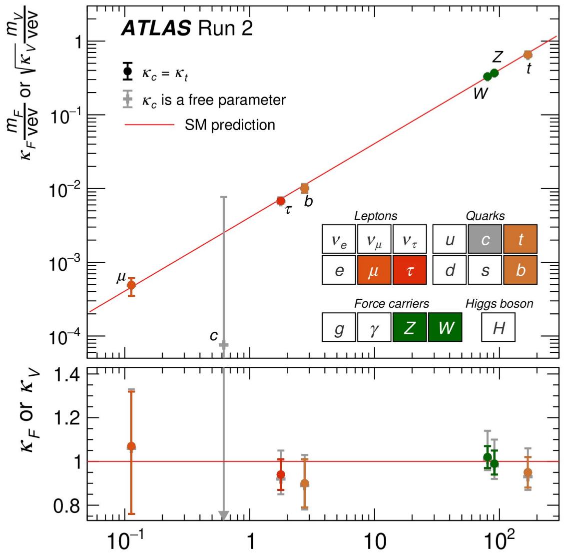

Nature 607, 52-59 (2022)

Higgs boson self coupling

- Di-Higgs boson production (*HH*) allows a direct access to Higgs boson self coupling, a crucial parameter of the Higgs mechanism
  → Difficult to probe since di-Higgs SM production rate is really low ($\sigma_H \simeq 2000 \times \sigma_{HH}$)
    - Multiple decay channels must be combined to look for it
      Main ones : *bbbb*, *bbττ* and *bbγγ*

arXiv:2406.09971v2

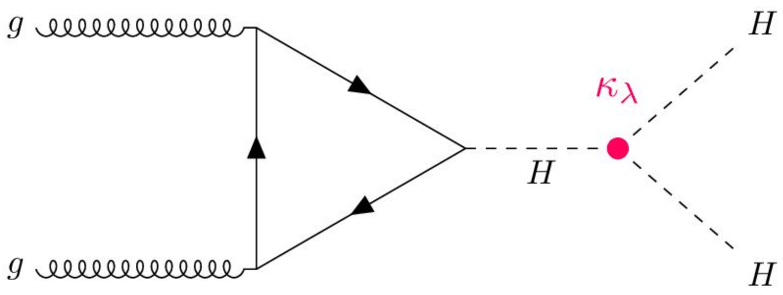

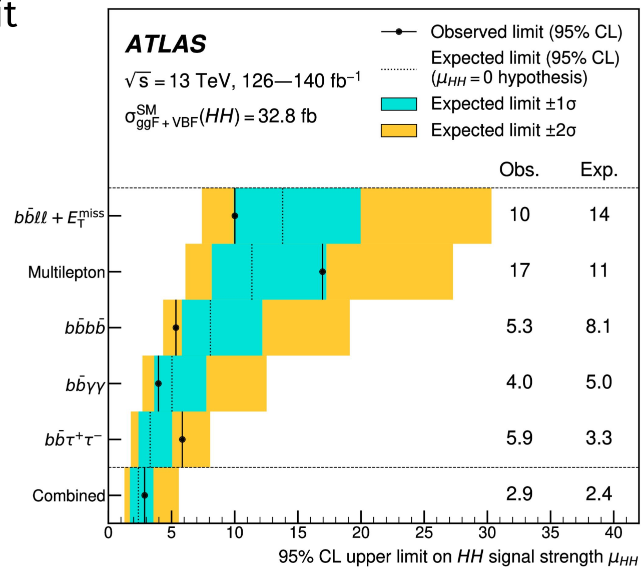

- For now only upper limits have been set but we look for any deviations from SM predictions as it could indicate new physics
  → Di-Higgs is an major objective for HL-LHC

Beyond Standard Model (BSM) physics

- The SM does not describe all phenomena and has some shortcomings :
  - Does not provide a dark matter particle candidate
  - Does not explain neutrino oscillation
  - The ‘Hierarchy problem’ coming from Higgs boson divergent radiative corrections

→ BSM physics consists in a variety of theoretical models that intend to fix (some of) the SM problems

- The Higgs sector is a promising place to look for BSM physics
  - Deviations from SM predictions could be observed in the Higgs properties
  - Some models (supersymmetry …) extend the Higgs sector by introducing new particles which could be directly detected at the LHC
    → additional scalar sector

e.g hMSSM exclusion limits
[ATL-PHYS-PUB-2024-008]

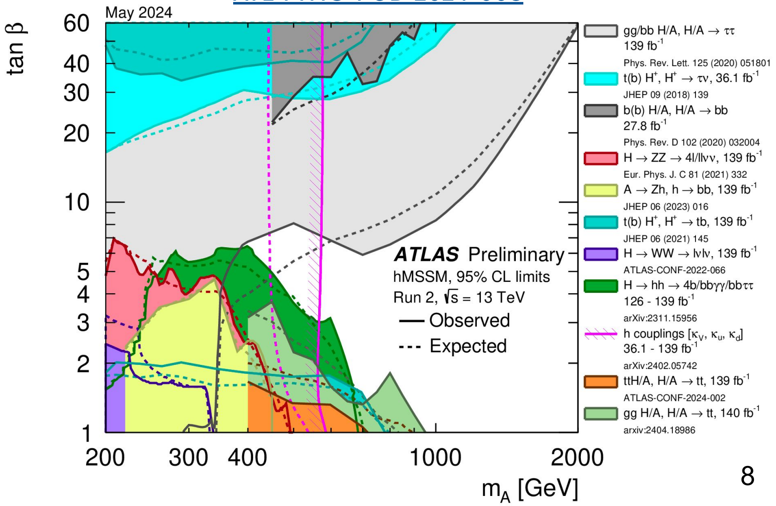

The ATLAS experiment

The Large Hadron Collider (LHC)

- The study of the Higgs boson requires high energy collisions

- This is done at the LHC at CERN
  - 27 km ring situated 100m underground
  - Proton-proton collisions up to 14 TeV
  - 4 detectors study the collisions : CMS, ALICE, LHCb and ATLAS
  - Different phases of operation :

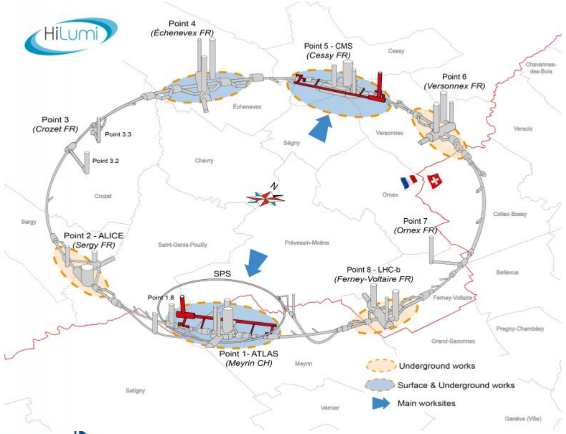

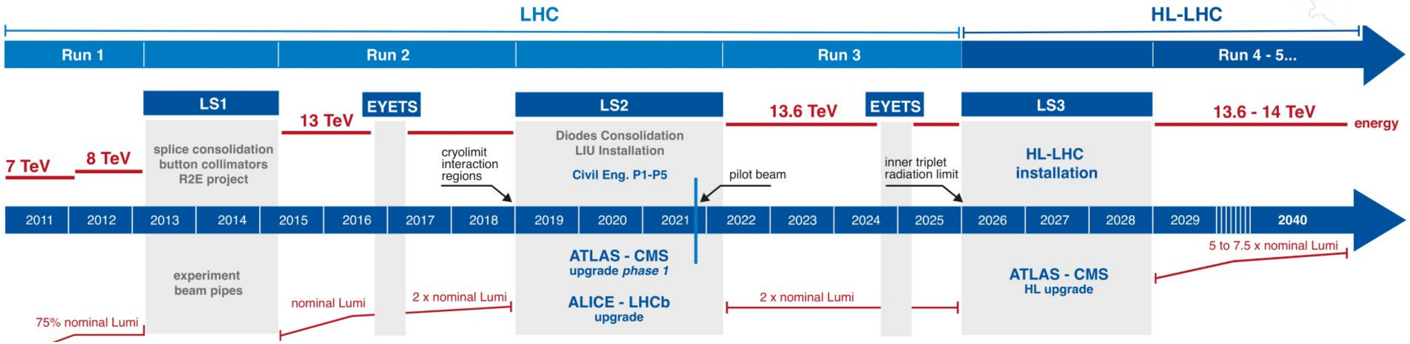

Run 2 (2015-2018) :
140 fb^{-1} of collisions at 13 TeV
Used for X →SH→bbγγ analysis

Run 3 (2022-2025) :
Already 149 fb^{-1} of
collisions at 13.6 TeV

High Luminosity (HL-LHC) (from 2029) :
expect 3000 fb^{-1} of 14 TeV collisions
Prospective *b*-tagging studies

The ATLAS Experiment

- ATLAS is a multipurpose detector that can study the Higgs boson, provide SM precision measurements and look for new physics

- 44m long, 25m tall, 7000 tons
  Four major components :
  - **Inner Detector** (ID) : trajectory reconstruction
  - **Electromagnetic** and **hadronic calorimeters** to measure particles energy
    → Photons and electrons reconstruction
    → Jet reconstruction (collimated stream of hadrons coming from a quark production)

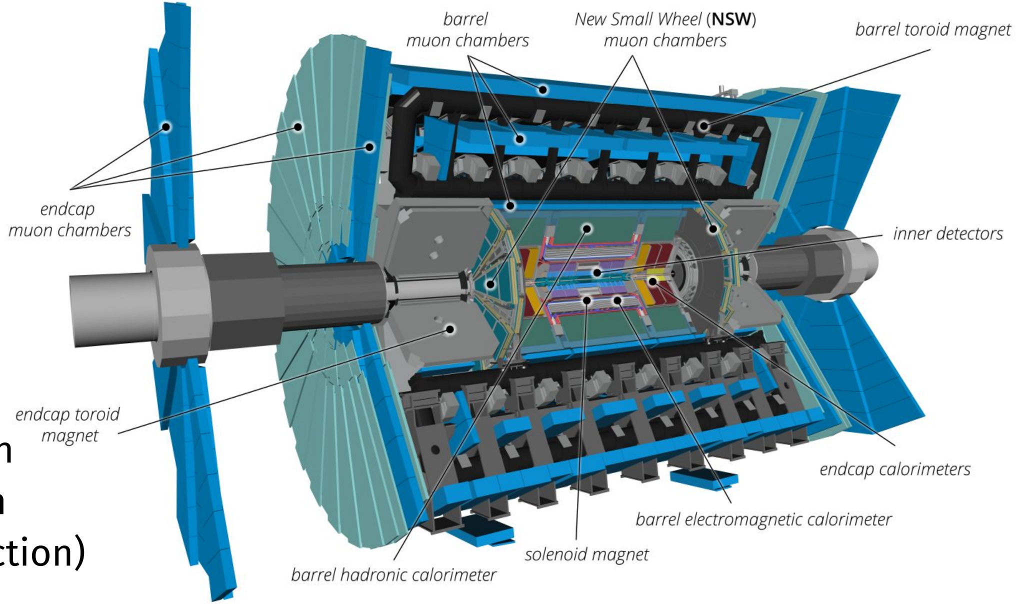

  - **Muon Spectrometer** to detect muons

  - **Magnet system** : bend charged particles trajectories and measure their impulsion

HL-LHC ATLAS and the Inner Tracker (ITk)

- The instantaneous luminosity will be increased during the HL-LHC era
→ More pile-up (i.e additional low energy interactions during beam crossings) :
from ~33 during Run-2 to up to 200 during HL-LHC
  - Busier environment (more tracks)
  - More radiation damage : HL-LHC fluence ~ 10 times larger than during Run 3

- The ATLAS detector will be upgraded and the ID will be replaced by ITk
  - 181 m² all-silicon detector with pixel and strip sensor types
  - Extended forward coverage from $|\eta|$ = 2.5 to 4

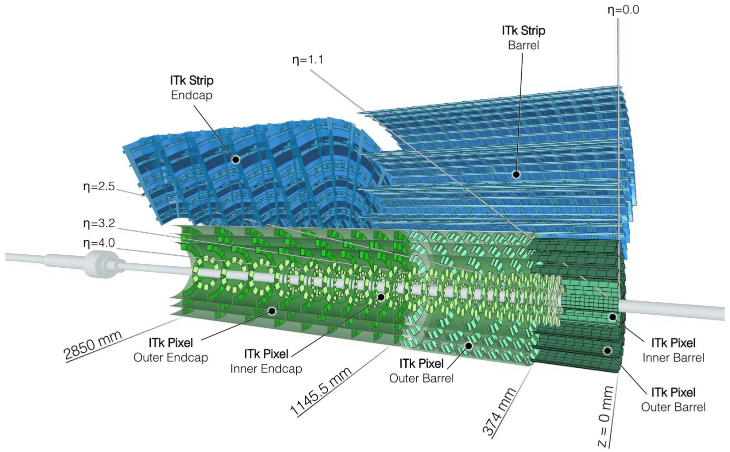

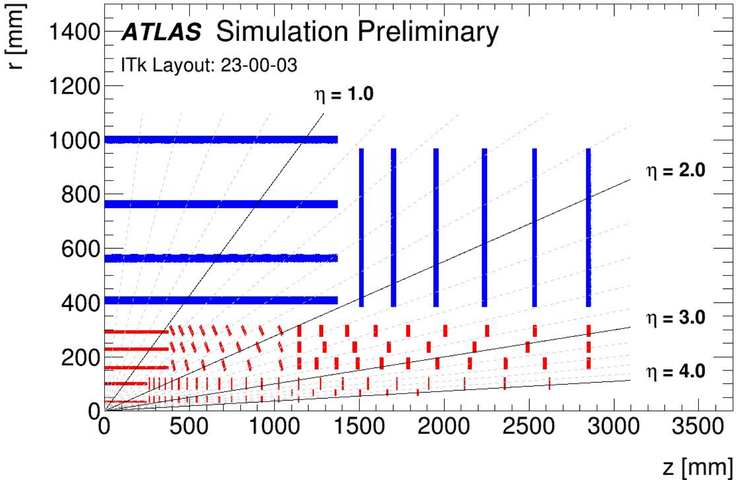

Adaptation of a neural network algorithm for flavour tagging at HL-LHC

Flavour tagging

- Flavour (or *b*) tagging is the process of identifying the flavour of the quark at the origin of a jet
  It is essential for Higgs physics and analyses with *b*-jets in the final state

- Use *b*-hadrons properties to identify *b*-jets :
  - Long lifetime → secondary vertex (SV) displaced from the primary vertex (PV)
  - Tracks coming from the SV have large transverse d_0 and longitudinal z_0 impact parameters (IP) with respect to the PV

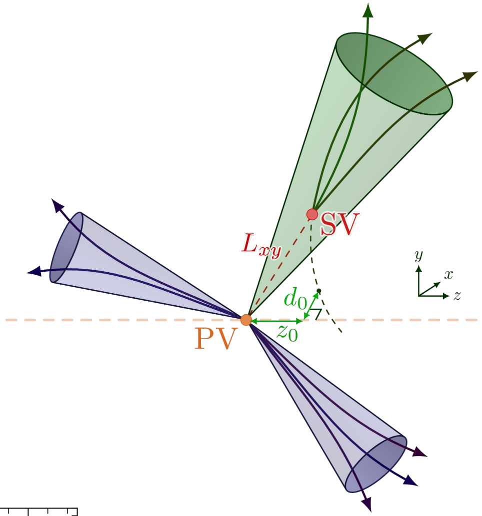

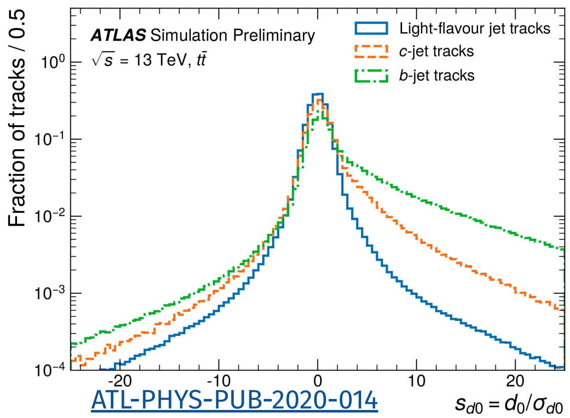

ATL-PHYS-PUB-2020-014

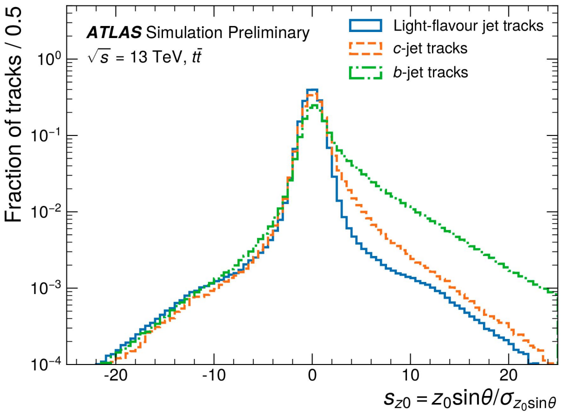

b-tagging algorithms in ATLAS

- ATLAS *b*-tagging algorithms :
  - 'Low' level algorithms (IP / SV based) - use IP/SV information separately
  - 'High' level algorithms - combine low level outputs to provide final *b*-tagging discriminant
  - More recently, GN1 is a graph neural network algorithm using tracks information

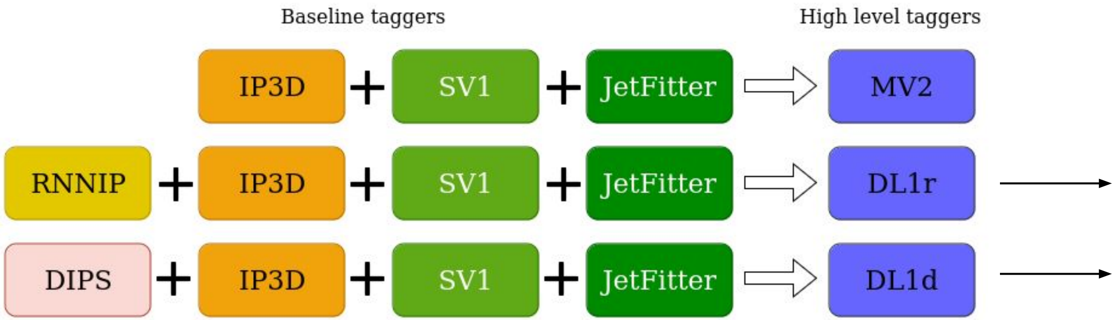

Used for full Run 2 analyses

Used for Run 2 analyses with Run 3 software

- **DIPS** is an impact parameter based algorithm
- Objective : train DIPS on the **ITk upgrade configuration**
  - Already done for older algorithms (IP3D, SV1, MV2)
  - Maintain (and possibly improve) *b*-tagging performance with harsher HL-LHC conditions

DIPS

- DIPS is a deep set neural network algorithm that takes tracks features as inputs
  They notably include the IP significances and the number of hits in certain layers of the detector

Track Input	Description
s_{d0}	d_0 / σ_{d0} : Lifetime signed transverse IP significance
s_{z0}	z_0 sin θ/ $\sigma_{z0 sin\theta}$: Lifetime signed longitudinal IP significance
log p_T^{frac}	log p_T^{track} / p_T^{jet} : Logarithm of fraction of the jet p_T carried by the track
log ΔR	Logarithm of opening angle between the track and the jet axis
nInnermostPixHits	Number of hits from the innermost pixel layer
nNextToInnermostPixHits	Number of hits in the next-to-innermost pixel layer
nInnermostPixShared	Number of shared hits from the innermost pixel layer
nInnermostPixSplit	Number of split hits in the innermost pixel layer
nPixHits	Number of pixel hits
nPixShared	Number of shared pixel hits
nPixSplit	Number of split pixel hits
nStripHits	Number of strip hits
nStripShared	Number of shared strip hits

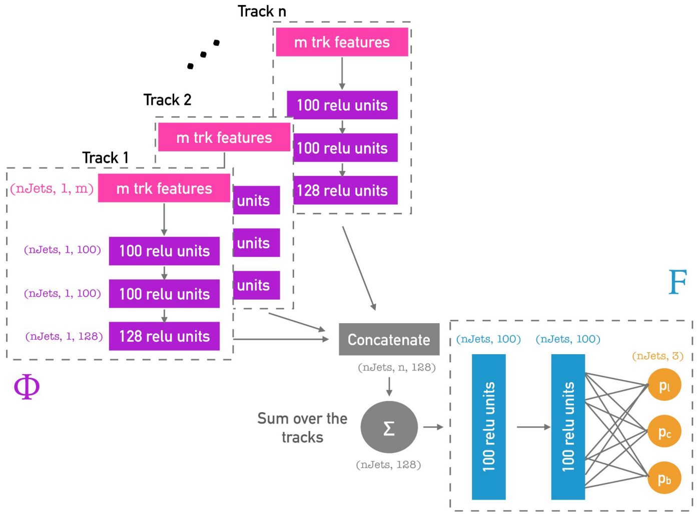

DIPS architecture

- A first network *Φ* handles each tracks inputs
- A second network *F* sums the different tracks and gives as an output the jet probability to be light / *c* / *b* flavoured

Jet selection

- Jet selection :
  - p_T > 20 GeV and $|\eta|<4$
  - Some selections criteria needed to emulate future upgrade performance :
    → Reconstructed jets must be matched to a true jet to remove pile-up jets
    → Good PV reconstruction criteria (|truth PV - reconstructed PV| < 0.1 mm)

- DIPS training is done with *tt* and *Z'* MC samples naturally rich in (*b*)-jets
  The training dataset is made of hybrid samples (70% *tt*, 30% *Z'*) designed to cover a large p_T spectra

p_T < 250 GeV
tt

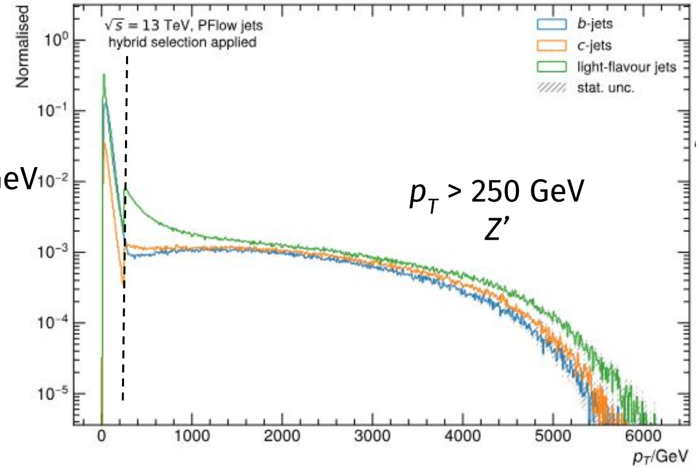

p_T > 250 GeV
Z'

Flavour	$t\bar{t}$	Z'	Total
b-jets	4.1M	650k	4.8M
c-jets	755k	700k	1.5M
light jets	4.9M	1.1M	6M

Flavour tagging performance

- Flavour tagging performance is evaluated with a ROC curve
  A discriminant is built from the algorithms output flavour probability $$D_{\text{DIPS}} = \log \frac{p_b}{(1-f_c)p_l + f_c p_c}$$
  where f_c balances light and c-jet rejection

ATL-PHYS-PUB-2020-014

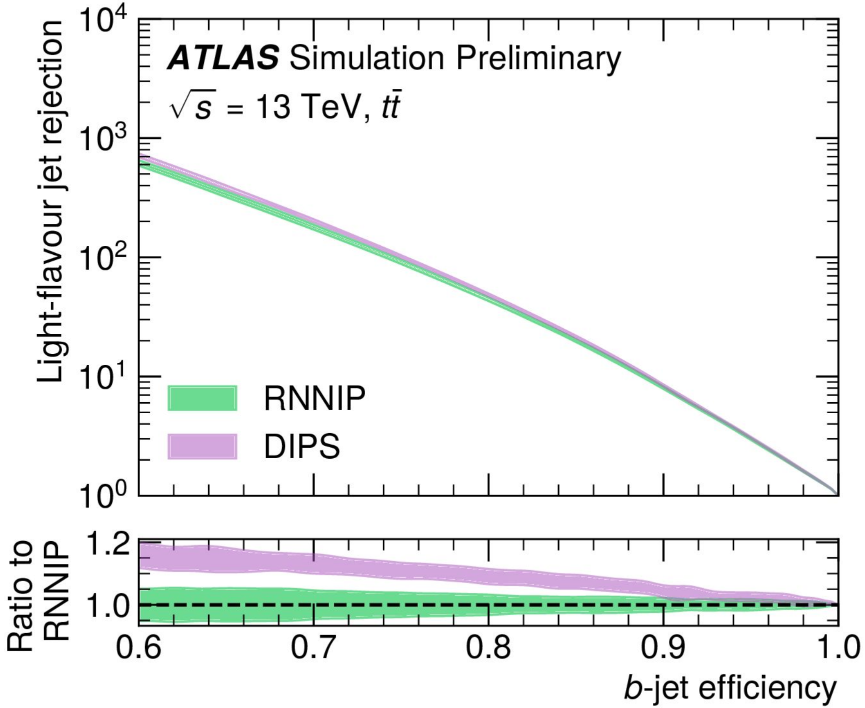

A threshold is determined on the discriminant distribution
→ All jets with a score above this threshold are tagged as *b*-jets, other ones are rejected

→ A ROC curve shows the *c* and light jet rejection as a function of *b* efficiency parameterised by the threshold value

Upgrade DIPS performance

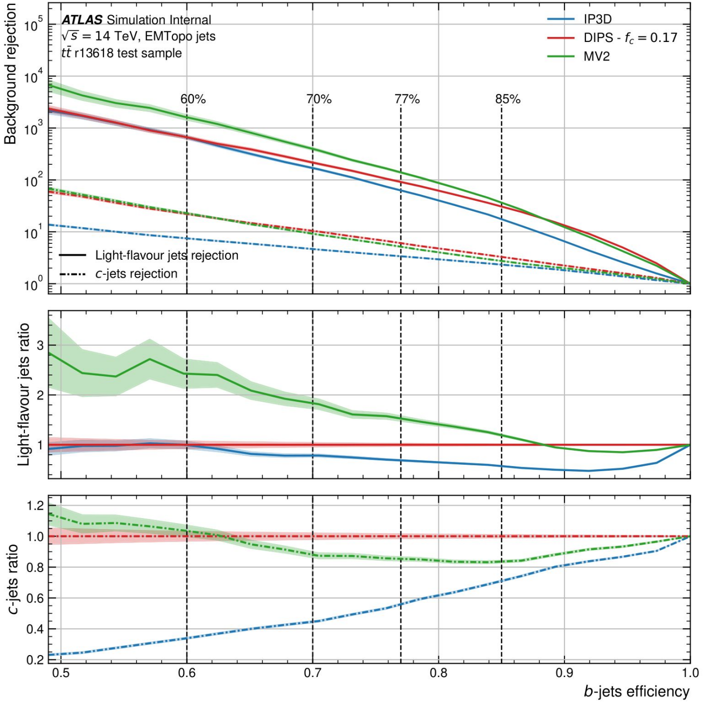

- DIPS performs much better than IP3D (older algorithm previously optimised for upgrade)

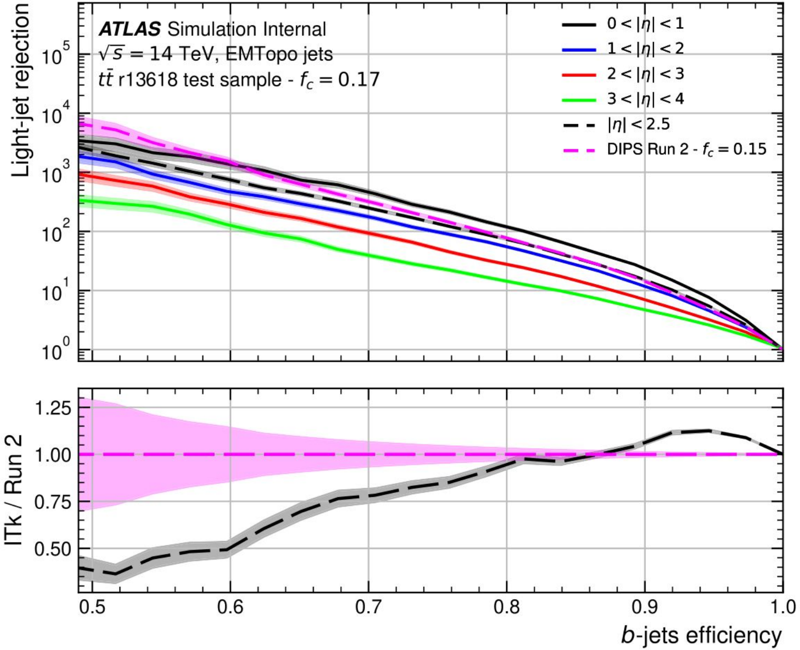

- DIPS performance degrades with η as expected because of the decreasing IP resolution
Performance is a bit worse than Run-2 DIPS in the central region

DIPS preprocessing and training

- The training dataset needs to have equal flavour repartition in p_T and η bins
  → this is obtained with a procedure called **resampling**

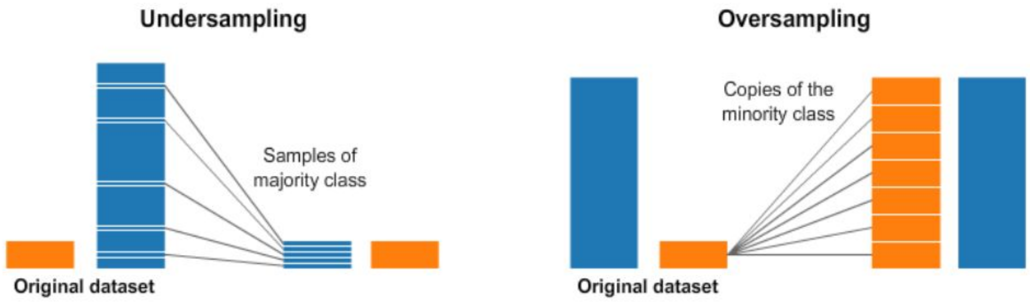

picture from Kaggle

- Two methods are tested :
  - **Count** / undersampling :
    scale the number of jets to the minority class (*c*-jets)
  - **pdf** : target *b*-jet distribution and use a mix of under and oversampling

- 3M training jets with count, 15M with pdf
  Keep current Run-2 DIPS architecture

Undersampling			
Flavour	$t\bar{t}$	Z'	Total
b-jets	755k	323k	1.07M
c-jets	755k	323k	1.07M
light jets	755k	323k	1.07M
			3.2M

pdf			
Flavour	$t\bar{t}$	Z'	Total
b-jets	3.5M	1.5M	5M
c-jets	3.5M	1.5M	5M
light jets	3.5M	1.5M	5M
			15M

Tracks selection

- The selection of the tracks used by the network can influence the performance
  A *Tight* and a *Loose* selection are defined and tested
  They differ by different selection criteria on p_T and transverse and longitudinal IP d_0 and z_0

Requirements	Tight tracks selection		
	$\|\eta\| < 2.0$	$2.0 < \|\eta\| < 2.6$	$2.6 < \|\eta\| < 4.0$
pixel + strip hits	≥ 9	≥ 8	≥ 7
pixel hits	≥ 1	≥ 1	≥ 1
pixel + strip holes	≤ 2	≤ 2	≤ 2
p_T [MeV]	> 1000	> 1000	> 1000
$\|d_0\|$ [mm]	≤ 1.0	≤ 1.0	≤ 1.0
$\|z_0 \sin\theta\|$ [mm]	≤ 1.5	≤ 1.5	≤ 1.5

Requirements	Loose tracks selection		
	$\|\eta\| < 2.0$	$2.0 < \|\eta\| < 2.6$	$2.6 < \|\eta\| < 4.0$
pixel + strip hits	≥ 9	≥ 8	≥ 7
pixel hits	≥ 1	≥ 1	≥ 1
pixel + strip holes	≤ 2	≤ 2	≤ 2
p_T [MeV]	> 900	> 500	> 500
$\|d_0\|$ [mm]	≤ 2.0	≤ 2.0	≤ 3.5
$\|z_0 \sin\theta\|$ [mm]	≤ 5.0	≤ 5.0	≤ 5.0

- Max. 40 tracks per jet

  Mean values :
  around 5 tracks / jet for *Tight*,
  around 7 tracks / jet for *Loose*

Results and trainings comparison

- The different tracks selection and resampling methods are compared :
  - *Loose* tracks selection better than *Tight*
  - pdf resampling method better than count
  - The *Loose* + pdf configuration provides the best performance

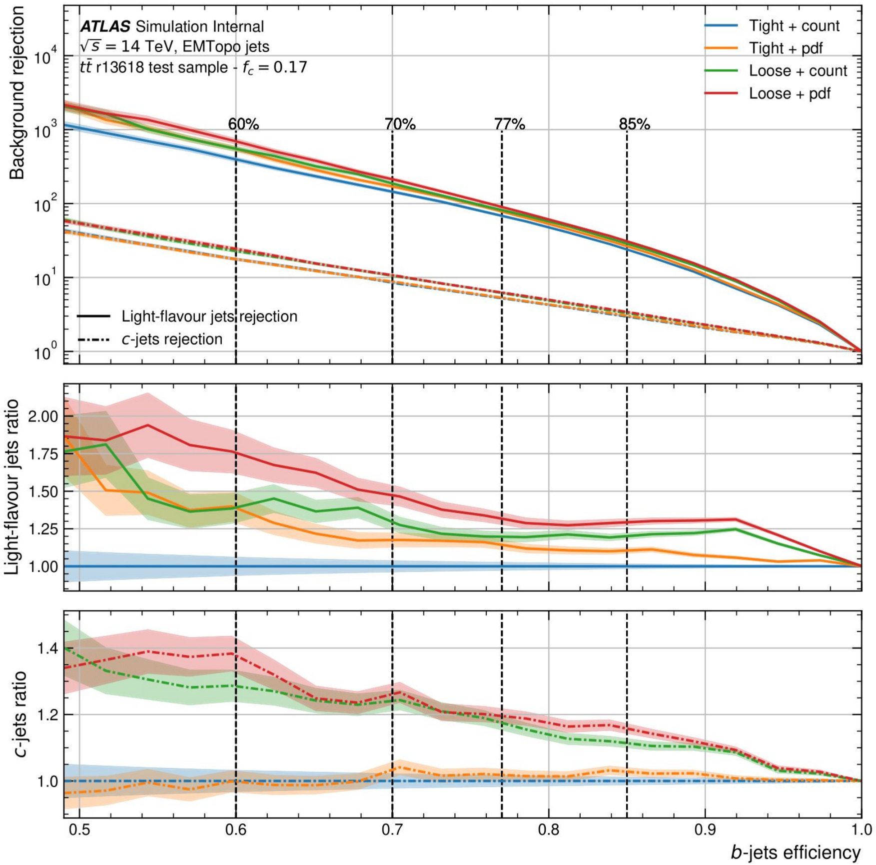

Global *b*-tagging performance in HL-LHC

- The selected DIPS model can then be used to perform an upgrade DL1d training
  The graph neural network based algorithm GN1 is also trained on the upgrade configuration
  Their performance is summed up in the ATL-PHYS-PUB-2022-047 ATLAS public note

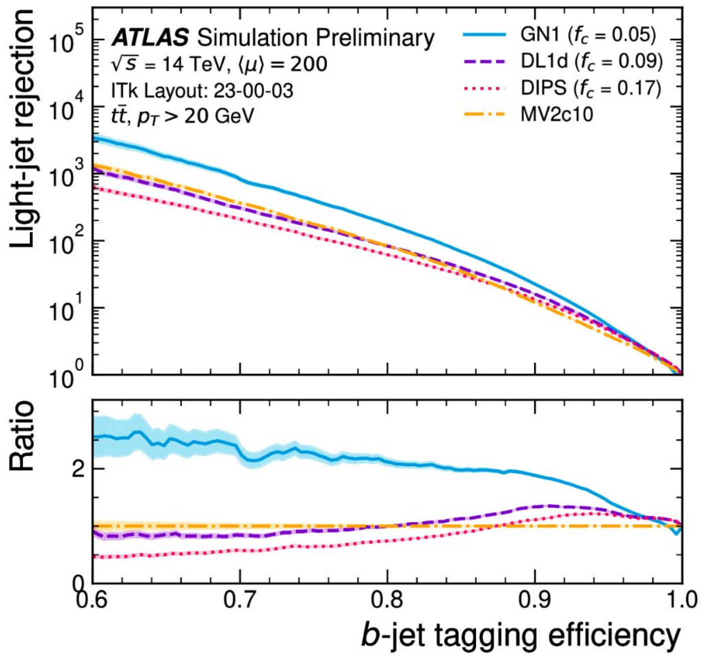

- 'All inclusive' graph neural network GN1 provides better results than the high level algorithm DL1d
  Future developments for flavour tagging at HL-LHC focus on the graph neural network approach

Search for two additional scalar particles in the $X \rightarrow S(\rightarrow b\bar{b})\ H(\rightarrow \gamma\gamma)$ channel

Analysis presentation

- This analysis targets an asymmetric decay $X \to S(\to bb)H(\to \gamma\gamma)$ where X and S are new scalar bosons. and H is the SM Higgs boson
  Some theoretical models predict this phenomenology :
  → 2HDM with a complex or scalar singlet, NMSSM, TRSM ...
  - The search is model independent in order to be as general as possible
  - Only assumption made is signal generation with narrow width approximation

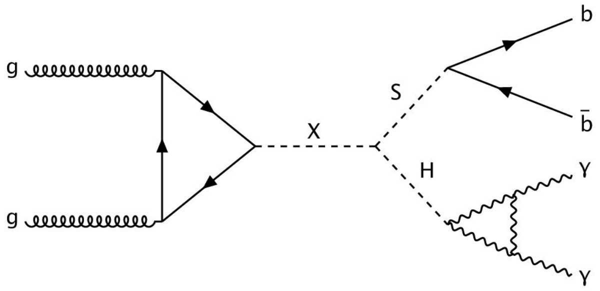

- Probed mass space :
  170 < m_X < 1000 GeV and 15 < m_S < 500 GeV

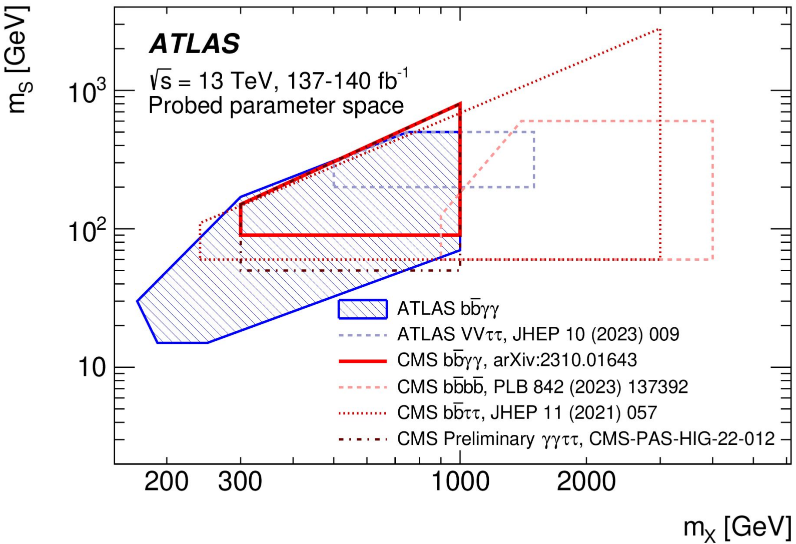

Dataset and event selection

- ATLAS Run-2 data (140 fb^{-1} at 13 TeV) is used

- Use diphoton trigger which requires event to have E_T > 35 (25) GeV for the leading (subleading) photon

- The event selection is :
  - Two '*Tight*' reconstructed and isolated photons which must also check
    105 < $m_{\gamma\gamma}$ < 160 GeV and $p_T(\gamma_1) > 0.35\, m_{\gamma\gamma}$ - $p_T(\gamma_2) > 0.25\, m_{\gamma\gamma}$ to target the $H \to \gamma\gamma$ decay

  - No lepton and between 2 and 5 central jets to reduce *ttH* background

  - One or two *b*-tagged jets at the 77% efficiency working point depending on the signal
    - The *b*-tagger used is DL1r

Different search regions

- A challenging situation arises when m_S << m_X: *S* is boosted and the *b*-jets coming from its decay are collimated and can be reconstructed as only one jet

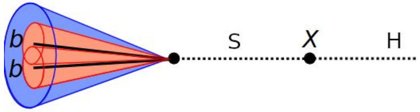

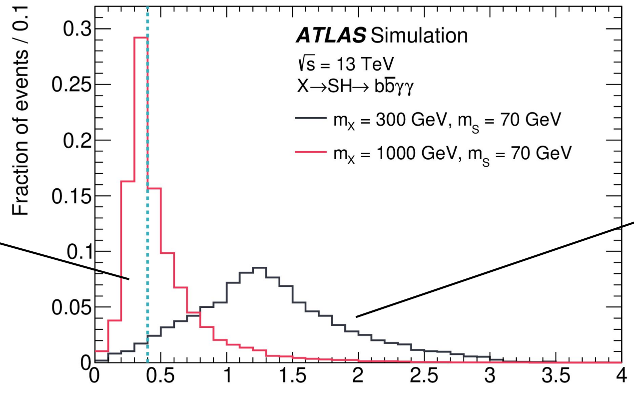

ΔR = 0.4 : standard angular size of reconstructed jets in ATLAS

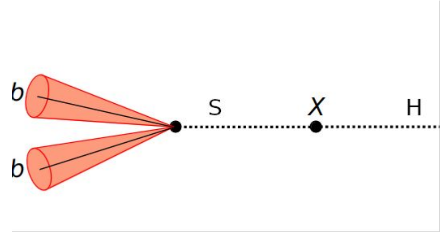

Fraction of events in the 2 b-tagged region

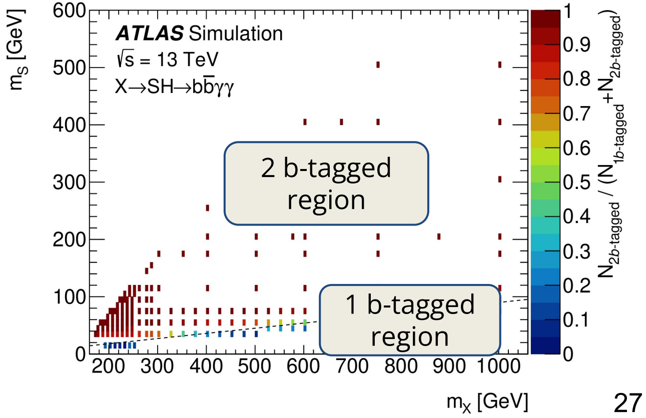

- The search space is separated between a **resolved region** with exactly 2 *b*-tagged jets and a **merged region** with exactly 1 *b*-tagged jet

The $bb\gamma\gamma$ channel

- Main backgrounds :
  - Non-resonant γγ+jets events
  - Resonant single Higgs : *ttH, ggH, ZH* and also *VBF H* in the 1 *b*-jet region

- Total number of selected events :

	1 b-tagged	2 b-tagged
HH	1.82 ± 0.27	1.68 ± 0.25
ttH	11.71 ± 1.1	8.12 ± 0.77
ZH	7.52 ± 0.17	3.64 ± 0.31
ggFH + $b\bar{b}H$	57.5 ± 43	6.64 ± 5.3
Other single Higgs	17.4 ± 10	1.97 ± 0.7
Non resonant $\gamma\gamma$+jets	16842 ± 122	1852 ± 40
Total	16936 ± 122	1874 ± 40

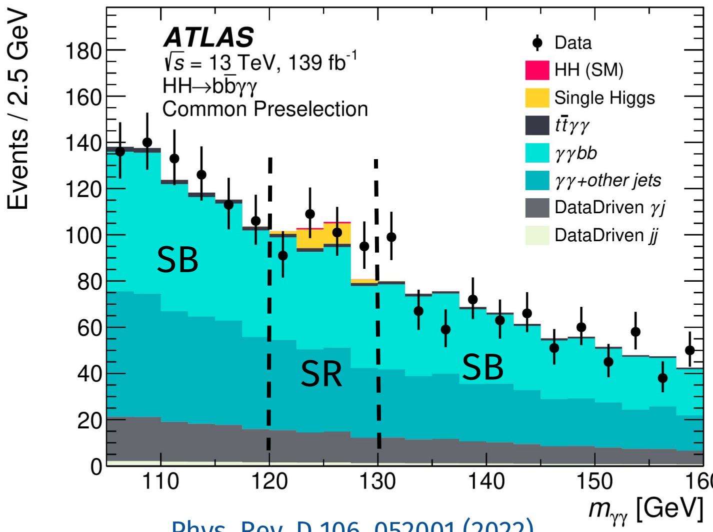

Phys. Rev. D 106, 052001 (2022)

- Use the $m_{\gamma\gamma}$ distribution to define :
  - A signal region (SR) between $120 < m_{\gamma\gamma} < 130$ GeV
  - Control region sidebands (SB) on the side

PNN discriminant

- Parameterised neural networks (PNN) are used to discriminate signal from background in the SR
  → They use a vector of parameters θ in addition to the input event features vector x

- One PNN in each signal region
  - 2 b-tagged region : $\theta = (m_S, m_X)$, $x = (m_{bb}, m_{bb\gamma\gamma}^*)$,
  - 1 b-tagged region : $\theta = (m_X)$, $x = (p_T^b, m_{b\gamma\gamma}^*)$

- Training includes events from both the SR and the SB
  Training samples :
  - γγ+jets, *ttH*, *ZH*, *ggH* and corresponding region signals
    VBF *H* and *HH* also included in the 1 b-tagged region

- PNN output is a score between 0 and 1

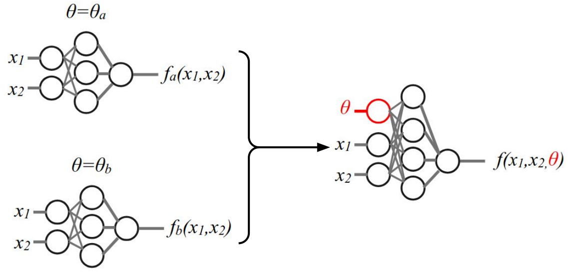

$$m_{bb\gamma\gamma}^* = m_{bb\gamma\gamma} - (m_{\gamma\gamma} - 125\text{ GeV})$$
$$m_{b\gamma\gamma}^* = m_{b\gamma\gamma} - (m_{\gamma\gamma} - 125\text{ GeV})$$

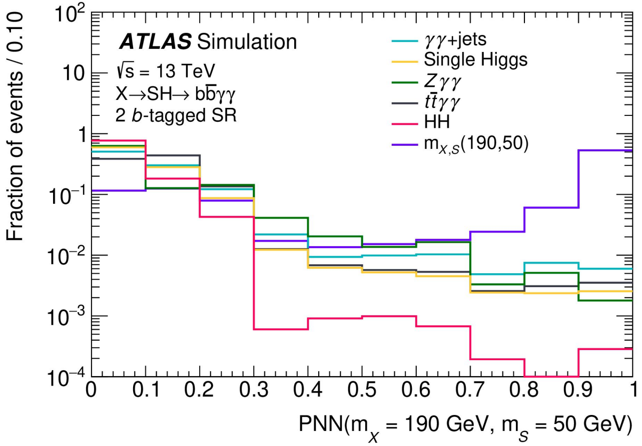

Background modelling and MC - data agreement

- Background PNN distributions come from MC samples
- Data - MC agreement in the PNN shape is checked in the SB
  The sideband distribution is used to normalize the γγ+jets process

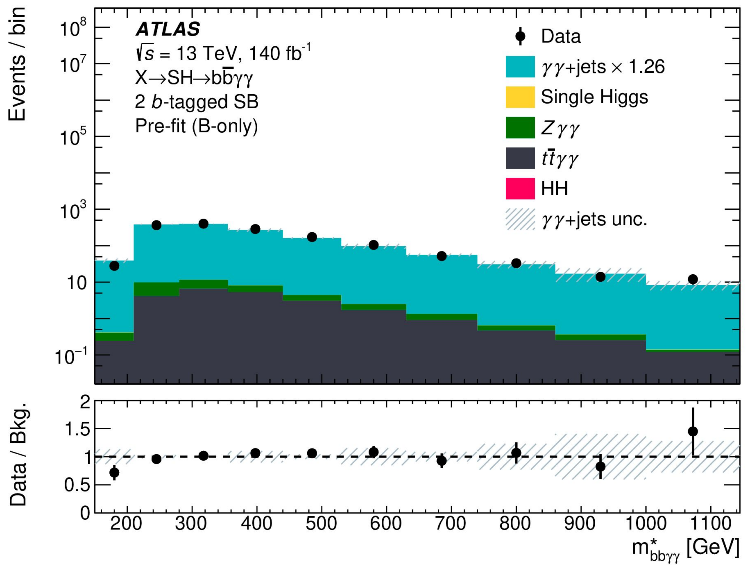

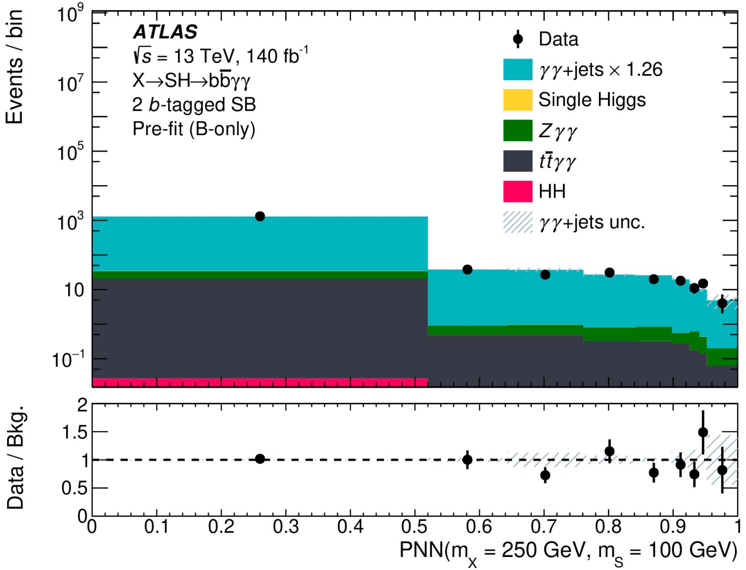

Systematic uncertainties

- Main sources of experimental systematic uncertainties include particle identification (e.g flavour tagging) and p_T and energy scale and resolution of the different objects
  - It changes the number of events in the SB and SR regions
  - It modifies the position and width of the peak in the m_{bb} and $m_{bb\gamma\gamma}$ distributions and eventually the shape of the PNN distribution

  Experimental systematics are computed with dedicated variables that give the calibrated ±1σ combined performance values
  → Taken into account for signal, major single Higgs, HH, $\gamma\gamma$+jets and $Z(qq)\gamma\gamma$ processes

- Theoretical systematic uncertainties :
  - SM parameters uncertainties (e.g α_S, QCD scale, branching ratio, PDF values)
    → Might affect processes production cross-section
  - Parton shower modelisation by the MC generator

Experimental systematic uncertainties - Background values

- Systematic uncertainties variations to the PNN distribution are categorised through yield and shape changes
  Yield changes reflect the impact on selection and change with respect to nominal value

	Source	Yield uncertainty (%) ttH	ZH	HH	ggH
Event-based	Photon Trigger	1.0	1.0	1.0	1.0
	Pile-up reweighting	0.9	0.8	0.6	0.4
Photon	Photon Energy Res.	0.4	0.4	0.3	0.4
	Photon Energy Scale	0.2	0.2	0.1	0.1
	Photon ID	1.6	1.6	1.4	1.6
	Photon Isolation	1.6	1.6	1.5	1.6
Jet	Jet Energy Scale	1.4	0.9	0.6	1.8
	Jet Energy Res.	7.3	4.6	2.9	7.5
Flavour-tagging	b-jet efficiency	2.1	3.0	2.5	3.1
	c-jet efficiency	0.4	0.7	0.1	1.7
	light-jet efficiency	0.8	0.4	0.4	2.7

- This table shows the yield relative difference with respect to nominal value (in %) for the **main background samples**
  NB : $\gamma\gamma$+jets normalization fixed by SB

- Major uncertainties are flavour tagging and jet energy resolution
  Relative difference remains below 10%

Experimental systematic uncertainties - Signal values

- For **signal**, the experimental systematic values depend on m_X and m_S
- Change is relatively constant for **photon systematics** because photons all come from the $H \rightarrow \gamma\gamma$ decay

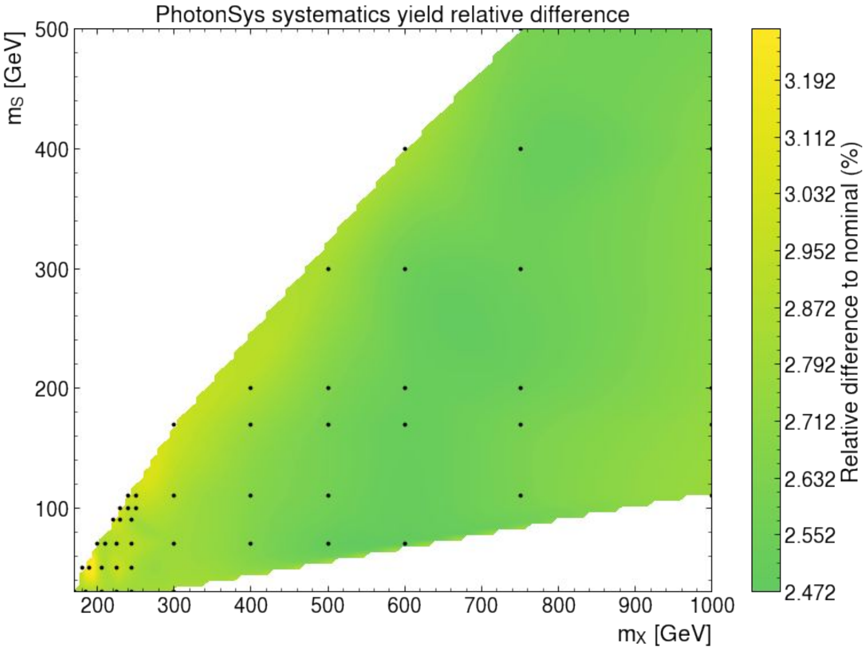

Experimental systematic uncertainties - Signal values

- Relative difference is higher at low mass for flavour tagging

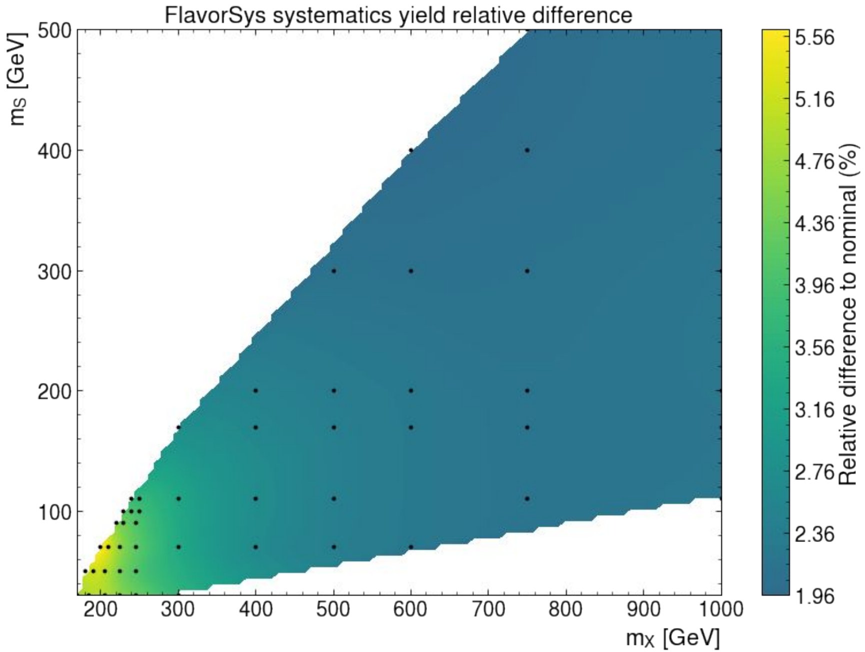

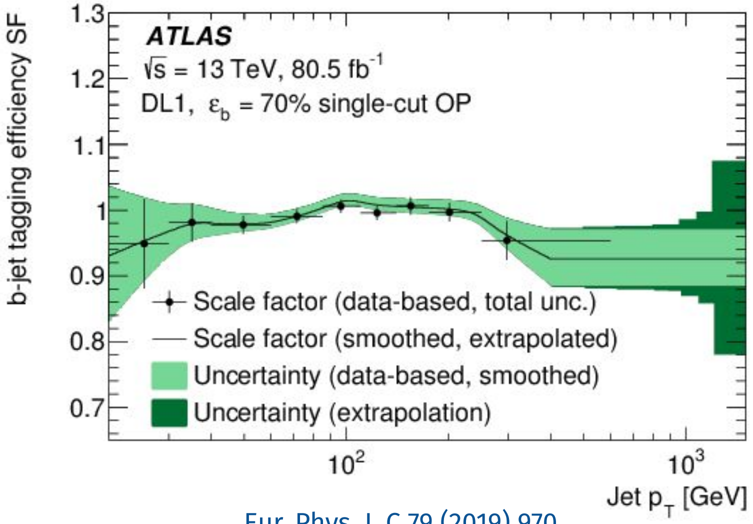

[Eur. Phys. J. C 79 (2019) 970]

- Lower mass → lower jet p_T → higher flavour tagging uncertainties

Experimental systematic uncertainties - Signal values

- Similarly, relative difference is higher at low mass for jet energy resolution

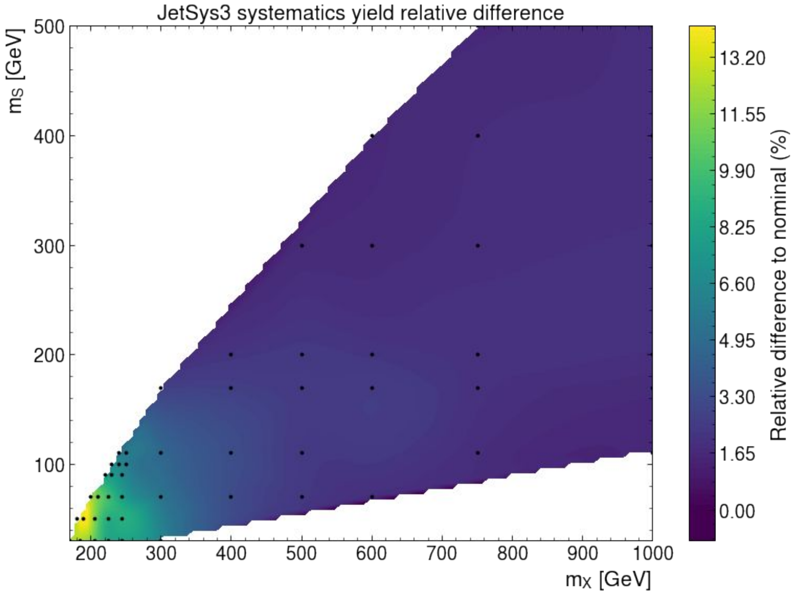

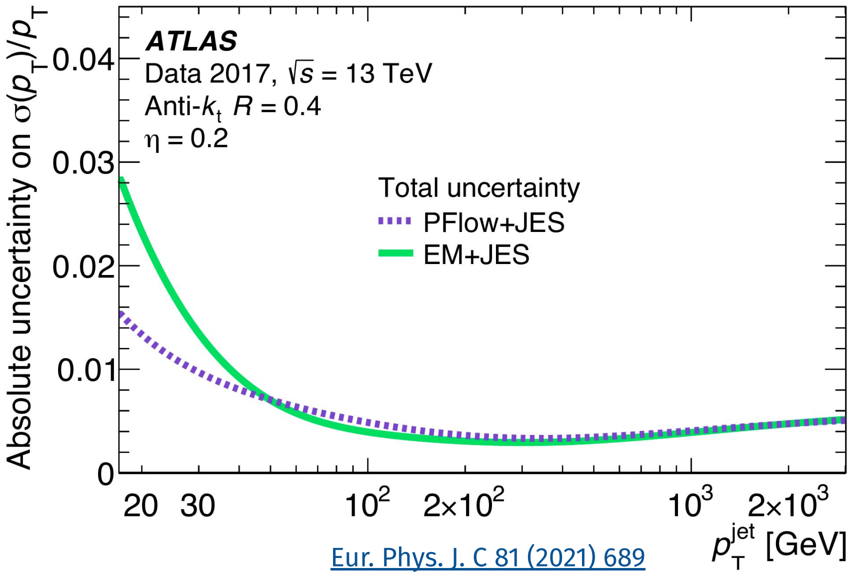

Eur. Phys. J. C 81 (2021) 689

- Lower mass → lower jet p_T → higher jet energy resolution uncertainties

Experimental systematic uncertainties - PNN shape variations

- Example of *shape* changes in the PNN distribution for one jet energy resolution uncertainty in the $\gamma\gamma$+jets and signal samples
  The variation in the last signal like bin doesn't exceed 10%

Signal

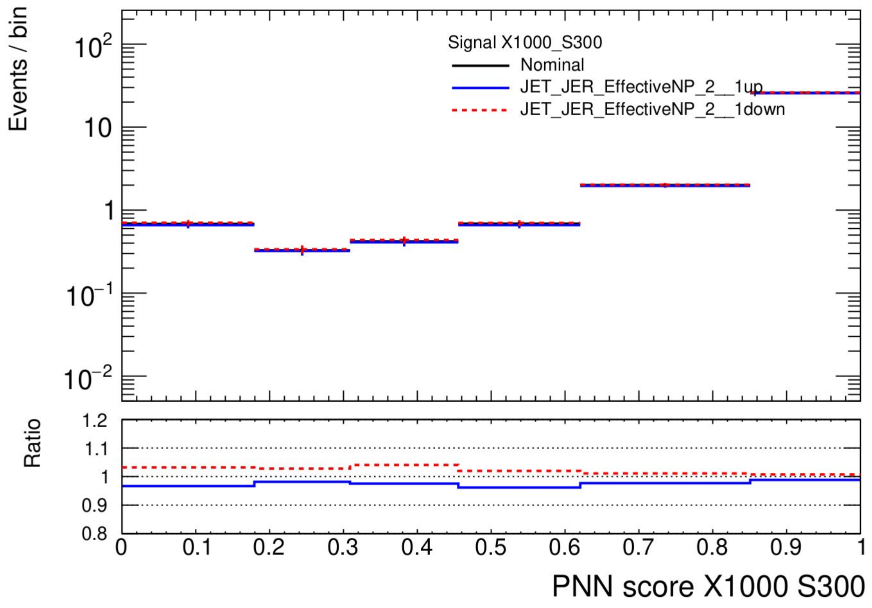

γγ+jets background

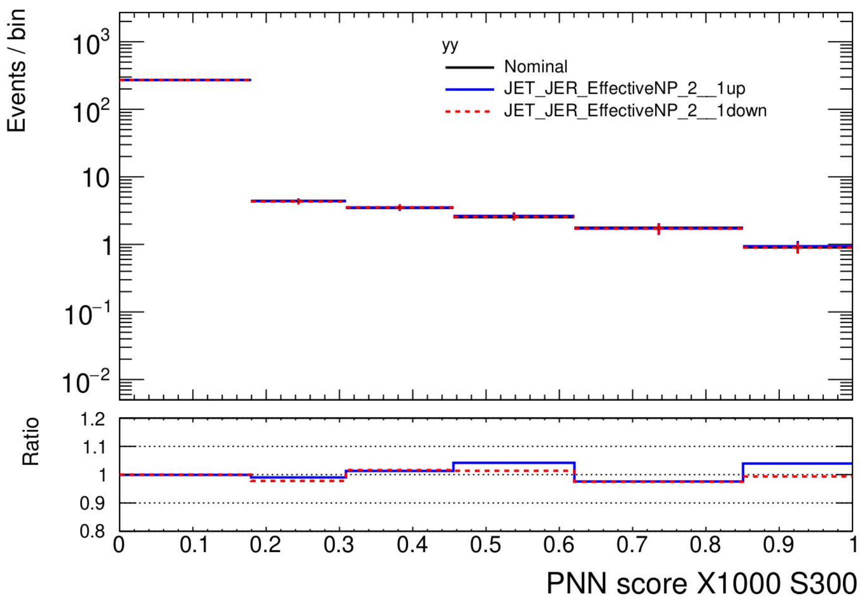

Analysis results

- Results are obtained with a binned likelihood fit on the PNN shape distribution

$\gamma\gamma$+jets normalisation is free parameter $\mu_{\gamma\gamma}$.

$f_i^p(\theta)$ PNN output shape

$$\mathcal{L} = \underbrace{\mathrm{Pois}\left(n_{\mathrm{SB}} \middle| \mu_{\gamma\gamma} N_{\mathrm{SB}}^{\gamma\gamma}(\boldsymbol{\theta}) + \sum_p N_{\mathrm{SB}}^p(\boldsymbol{\theta})\right)}_{\substack{\textit{Data vs Bkg model yield in the} \\ \textit{single bin } m_{\gamma\gamma} \textit{ \textbf{sideband}}}} \cdot \underbrace{\prod_i \mathrm{Pois}\left(n_{\mathrm{SR},i} \middle| \underbrace{\mu_{\gamma\gamma} N_{\mathrm{SR}}^{\gamma\gamma}(\boldsymbol{\theta}) f_i^{\gamma\gamma}(\boldsymbol{\theta})}_{\gamma\gamma\text{+jets}} + \underbrace{\sum_p N_{\mathrm{SR}}^p(\boldsymbol{\theta}) f_i^p(\boldsymbol{\theta})}_{\textit{Processes other than } \gamma\gamma\textit{+jets}}\right)}_{\substack{\textit{Data vs model yield in the multi-PNN} \\ \textit{bins inside the \textbf{signal region}}}} \cdot G(\boldsymbol{\theta})$$

θ : nuisance parameters

- Systematic uncertainties are taken into account in the fit as nuisance parameters

Analysis results - Experimental uncertainties impact

- Systematic uncertainties impact can be assessed by comparing **blinded** limits obtained when they are taken into account to when they are not

Impact at low m_X

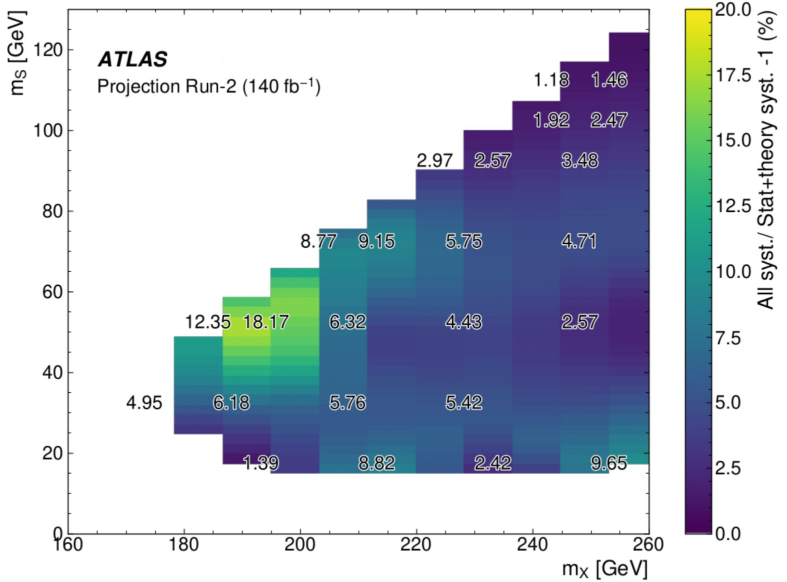

Impact at high m_X

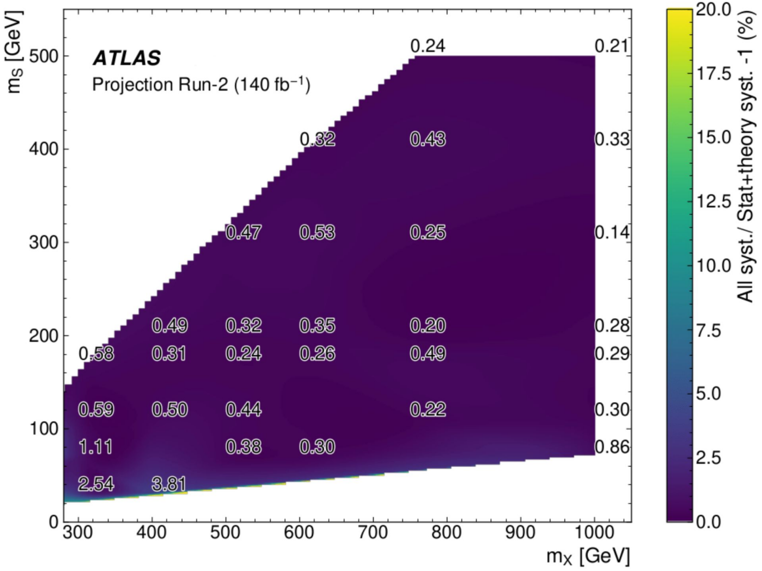

- Experimental uncertainties impact is really low at high mass (below 1%) but can reach 20% at low mass due to large signal uncertainties

Analysis results - Signal significance

- Discovery statistical tests are performed for every considered mass point
  The largest excess with respect to the background only hypothesis is observed for (m_X, m_S) = (575, 200) GeV
  Local (global) statistical significance is 3.5σ (2.0σ)
- No excess is noticed for (m_X, m_S) = (650, 90) GeV where CMS observed a local (global) 3.8σ (2.8σ) deviation

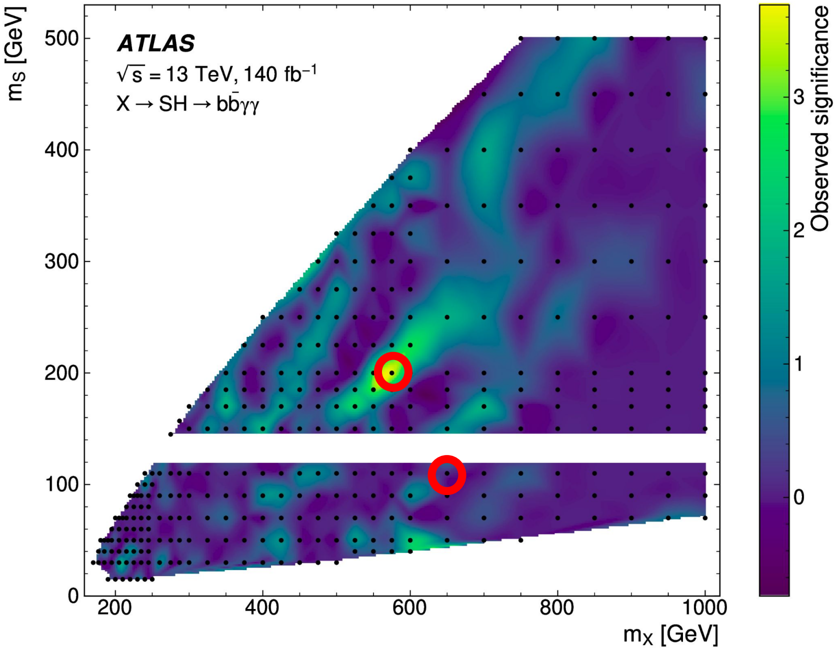

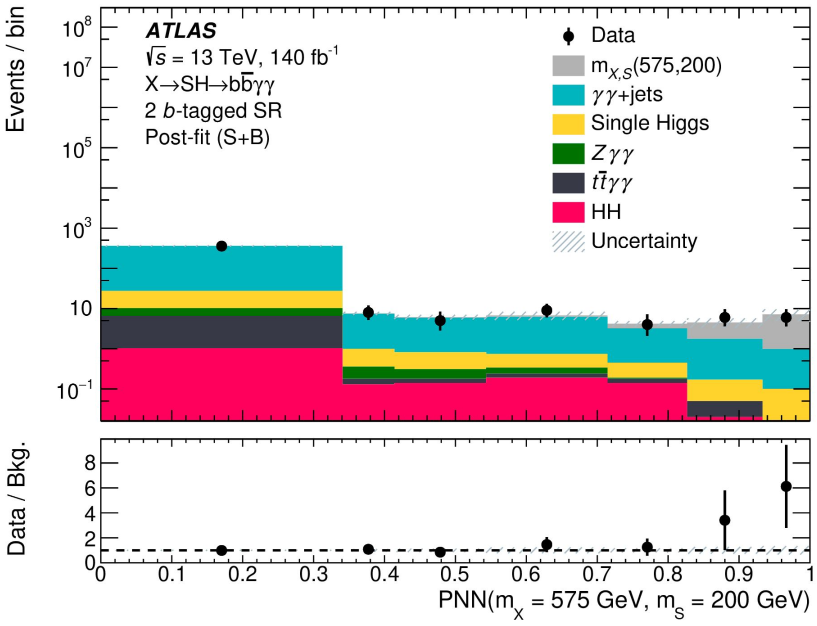

Analysis results - Limits

- Limits are set on the production cross section times *bbγγ* branching ratio in the mass space

Limits at low m_X

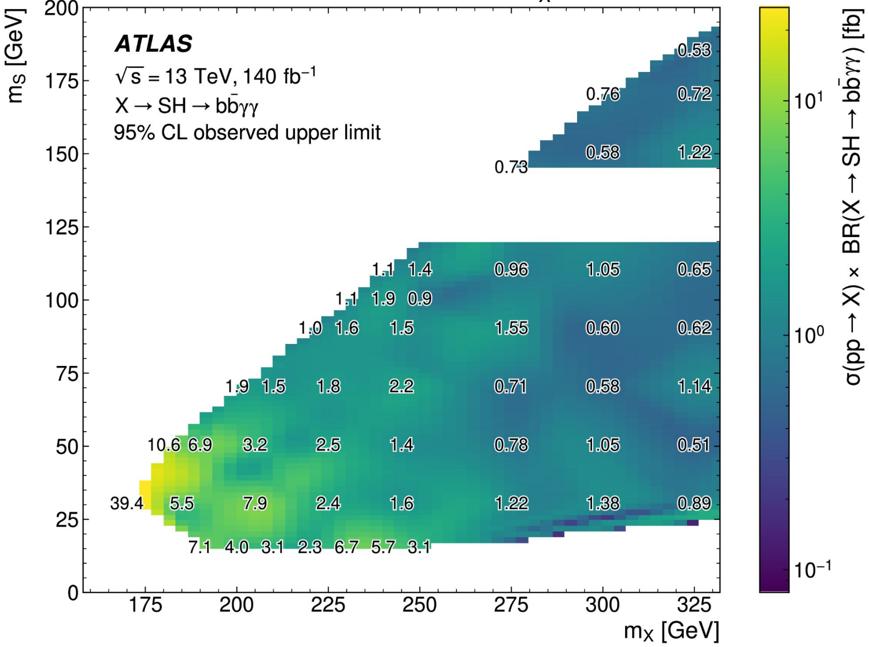

Limits at high m_X

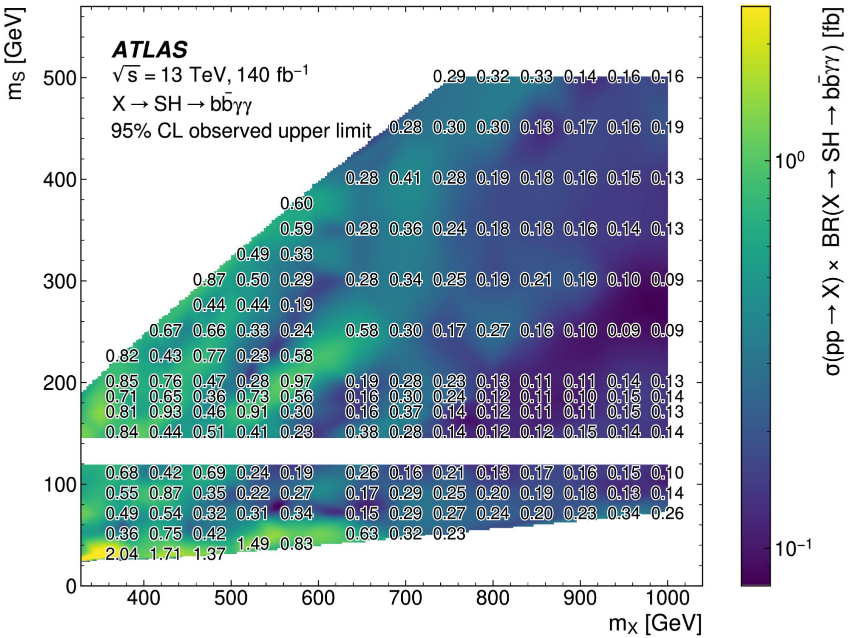

- Limits range from 0.09 fb at high mass to 39 fb at low mass
  Best sensitivity achieved in the high mass region thanks to a better signal efficiency

Analysis perspective

- The analysis has been submitted to JHEP
  Preprint is already available arXiv:2404.12915

- New perspectives will be offered with the upcoming Run 3 data
  - Already more statistics than Run 2, which will allow to shed more light on the observed excesses

  - The analysis techniques developed for the *bbγγ* final state can be useful for the *HH* research in the same channel

Conclusion

- Training of a *b*-tagging neural network algorithm with the HL-LHC configuration
  - Run 3 and HL-LHC will greatly increase the available data statistics
    → Crucial to study and optimize future detector performance
  - DIPS obtains better performance compared to previous upgrade studies
  - Future developments will focus on the graph neural network approach

- Research of two additional scalar bosons in the $X \rightarrow SH \rightarrow bb\gamma\gamma$ channel
  - First analysis to probe an uncharted phase space for low m_S and m_X values
  - Systematic uncertainties impact is assessed over the whole mass space
  - Largest deviation of 3.5σ (2.0 global) at (m_X, m_S) = (575, 200) GeV
    → No deviation observed for CMS 3.8σ local excess at (m_X, m_S) = (650, 90) GeV
  - Limits from 0.09 to 39 fb are set on the production cross section in the $bb\gamma\gamma$ channel

Backup

Di-Higgs production

- Interfering ‘triangle’ and ‘box’ diagrams for ggF HH production - $\sigma_{\text{ggF}}(HH)$ = 31 fb

Phys. Rev. D 106, 052001 (2022)

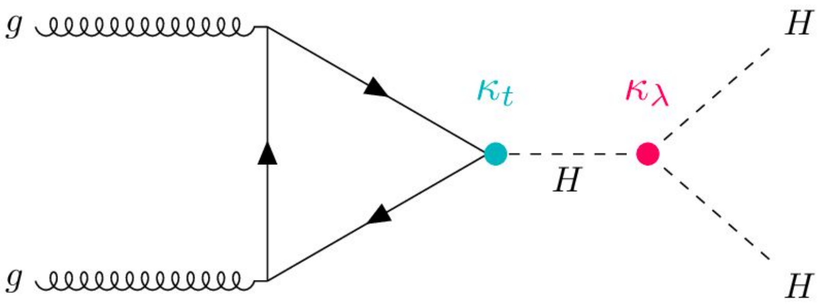

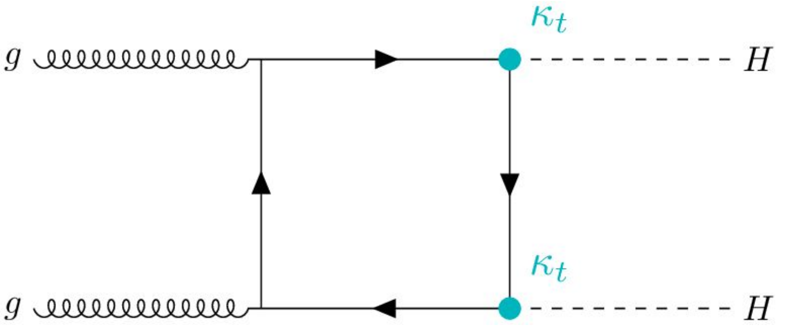

- VBF HH production also allows to probe κ_V and κ_{2V} - $\sigma_{\text{VBF}}(HH)$ = 1.73 fb

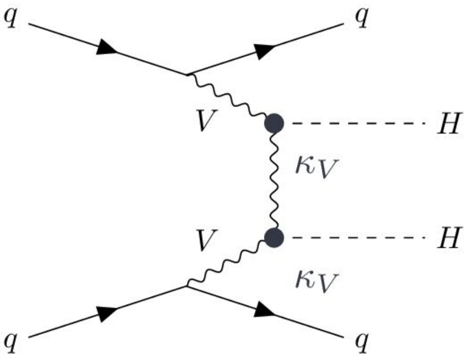

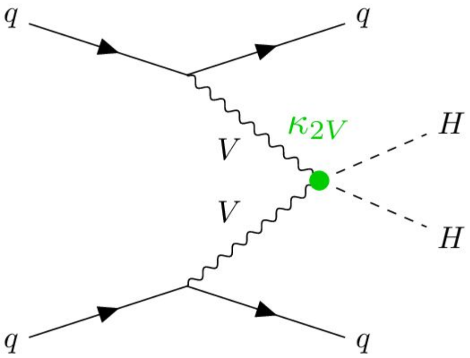

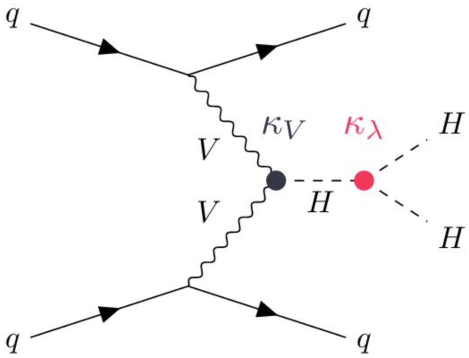

Luminosity and pile-up at (HL)-LHC

- Mean pile-up throughout LHC runs - latest plot available [here]()

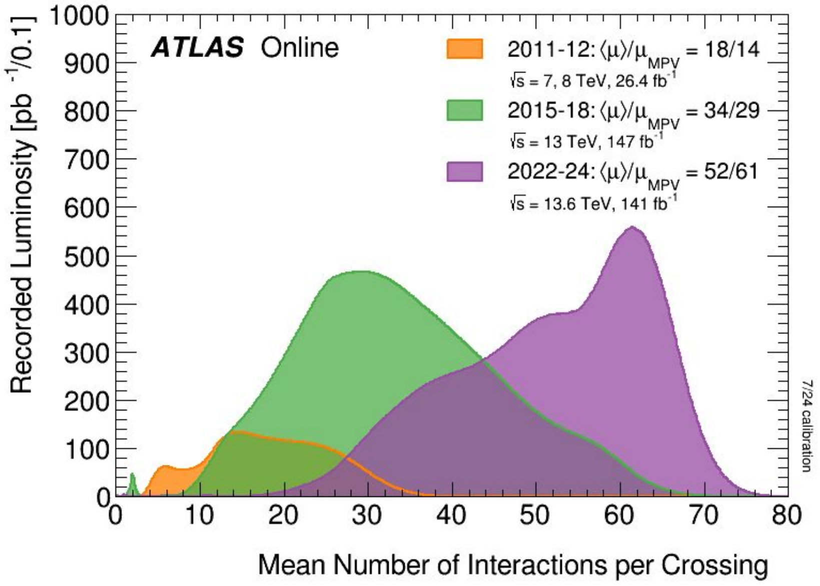

- Integrated luminosity per year

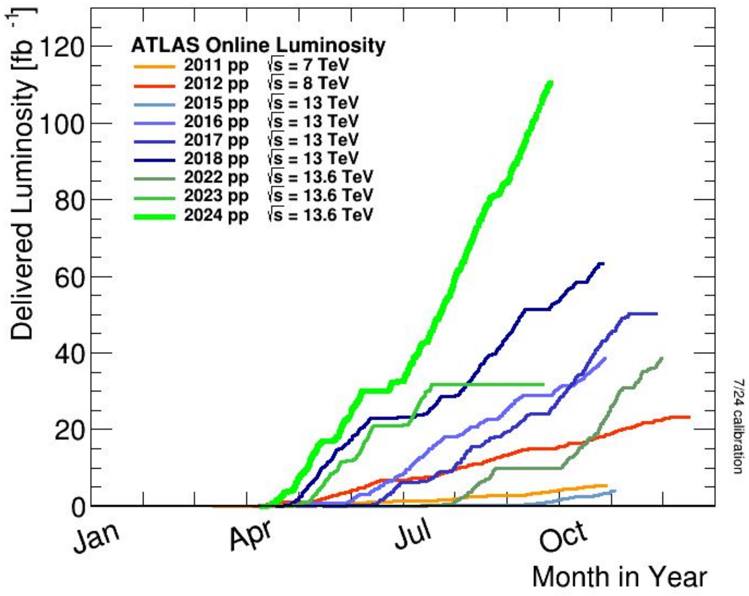

ITk tracking dependence in |η|

- ITk material distribution expressed in radiation lengths (X_0) in function of pseudorapidity |η|

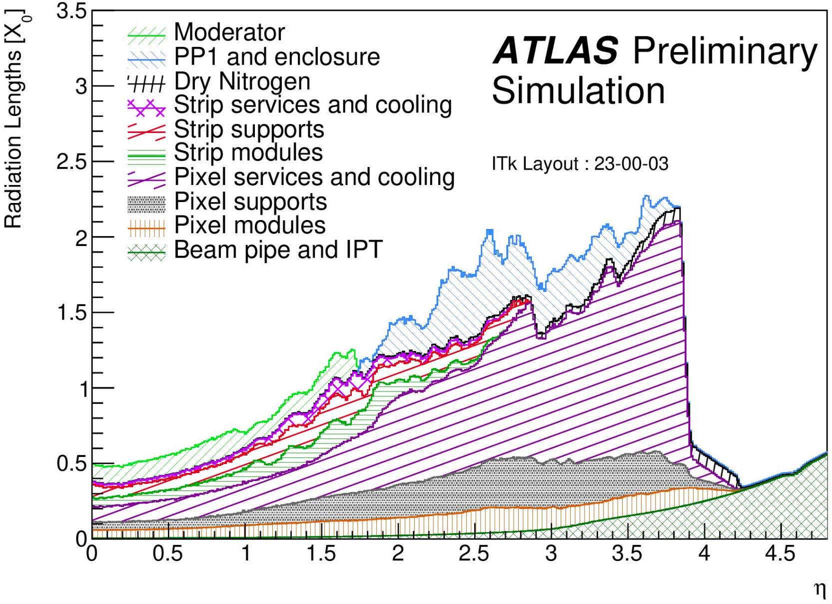

ATL-PHYS-PUB-2021-024

- Transverse IP resolution as a function of |η|

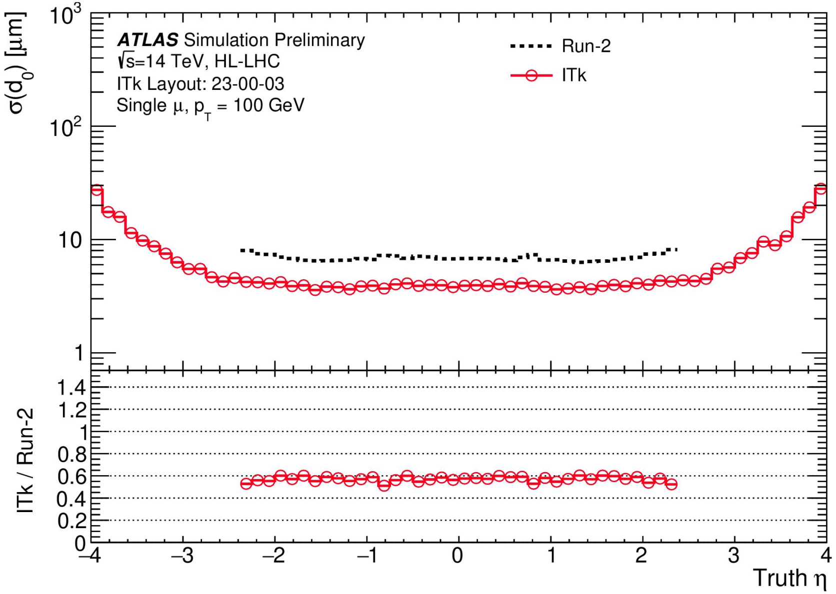

DIPS tracks inputs

- Distribution of the number of tracks per jet in the *Tight* (left) and *Loose* (right) tracks selection

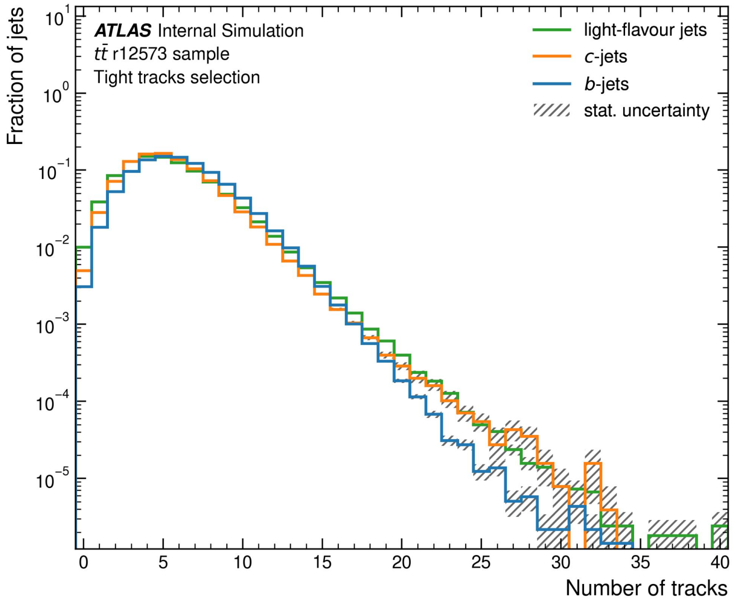

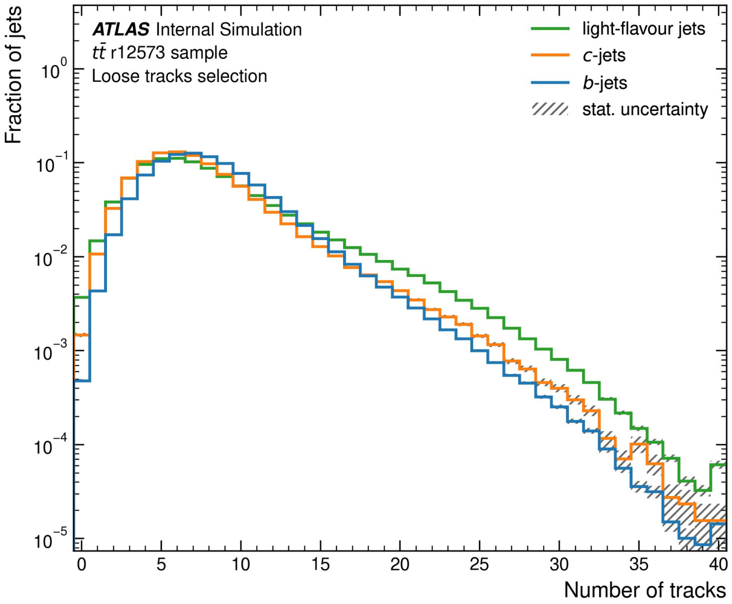

DIPS tracks inputs

- Tracks origin in *tt* samples for *Tight* (left) and *Loose* (right) tracks selection (flavour inclusive)

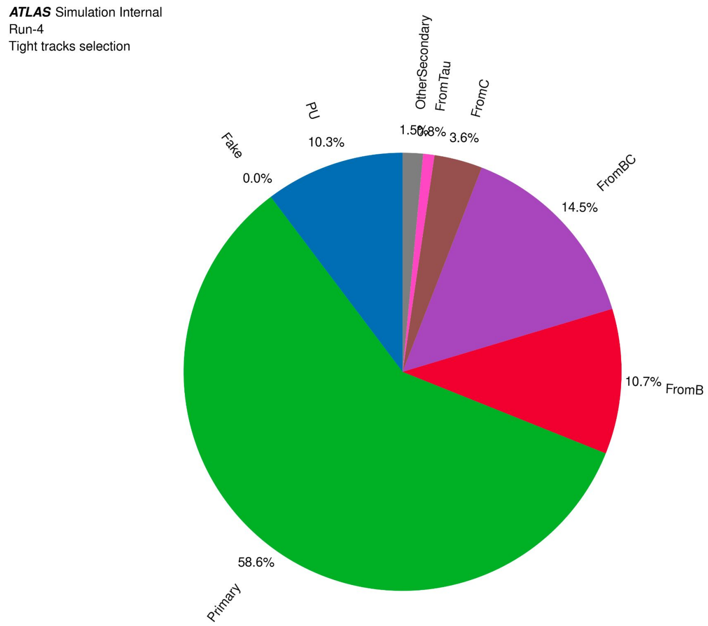

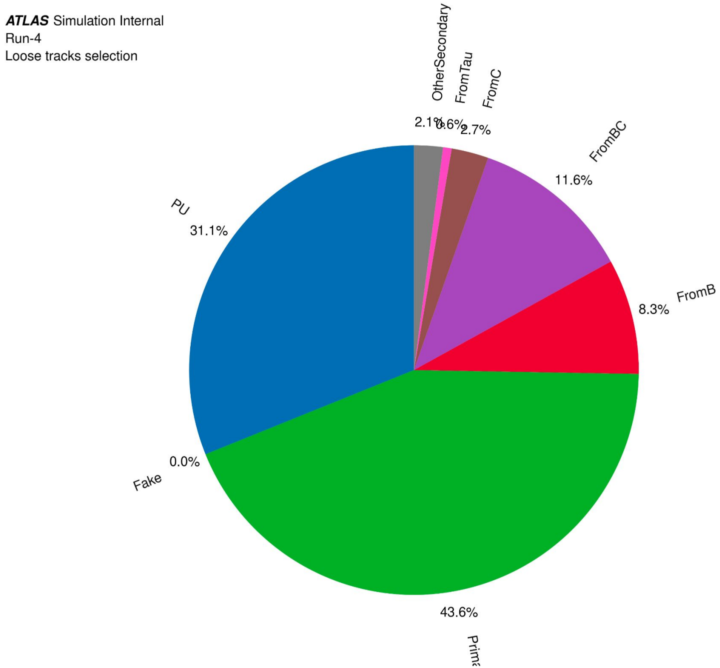

DIPS upgrade training metrics

- Training loss evaluated on the training and validation sets

Count training w/ *loose* tracks selection

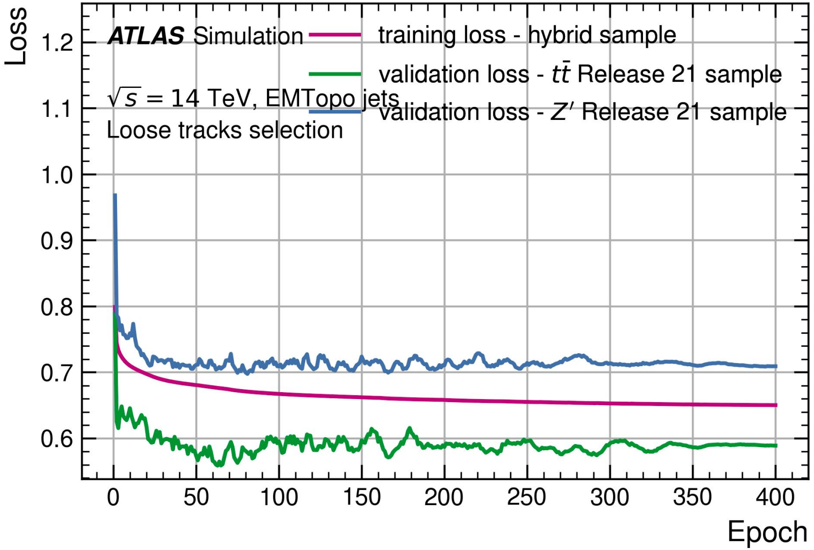

pdf training w/ *loose* tracks selection

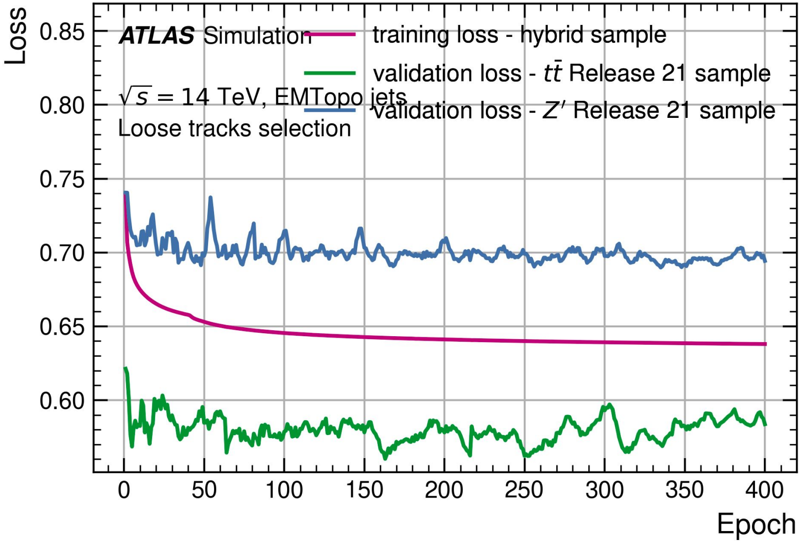

Upgrade DIPS additional performance plots

- Performance evaluation on *Z'* samples (probes high p_T jets)

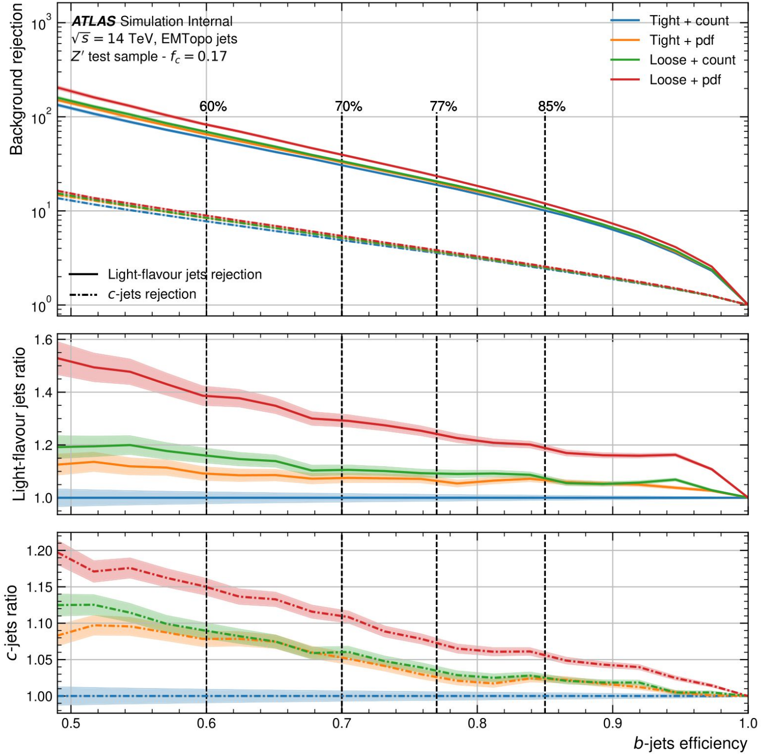

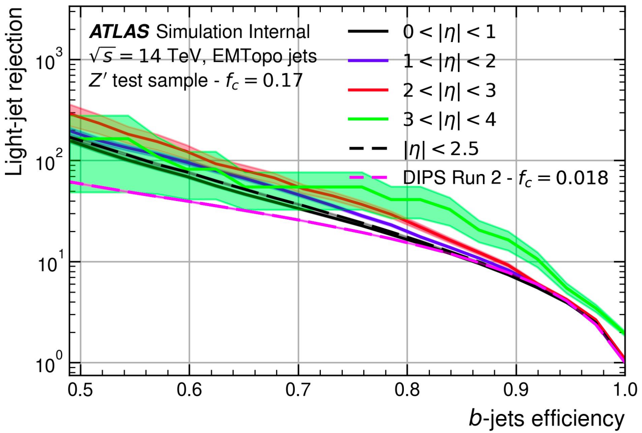

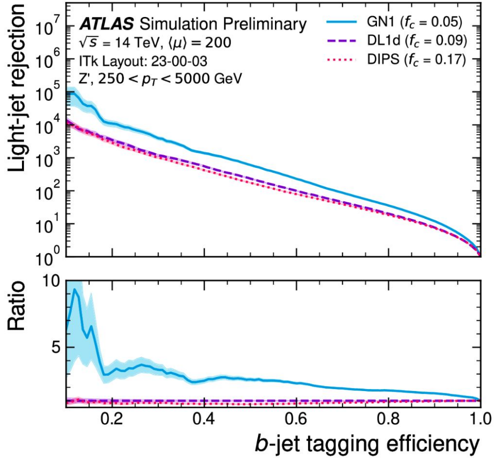

Upgrade DIPS additional performance plots

- Performance p_T dependence

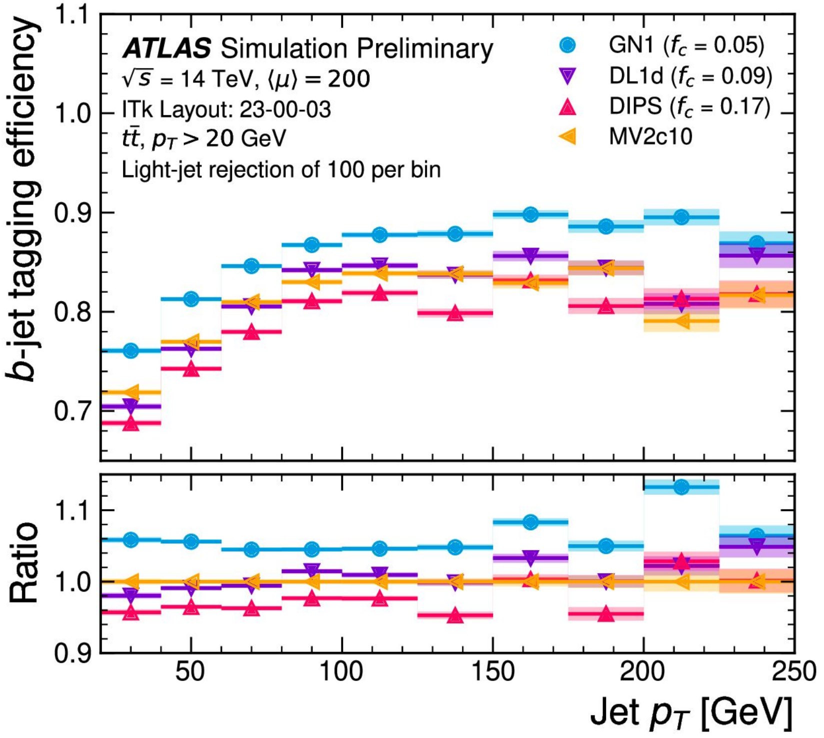

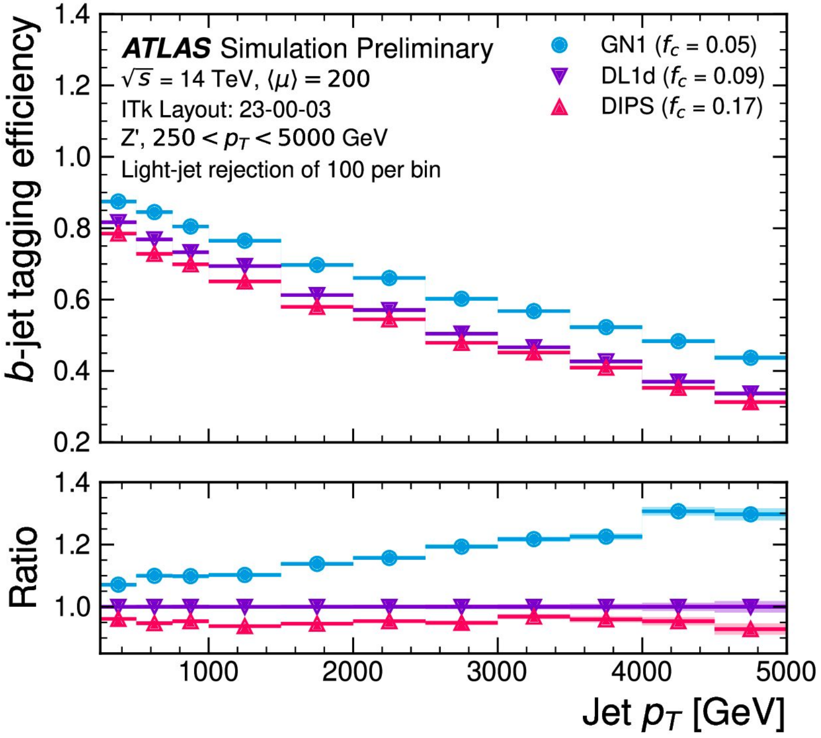

Upgrade DIPS additional performance plots

- Fraction scan plots shows the balance between light and *c*-jet rejection with curves parameterized by f_c

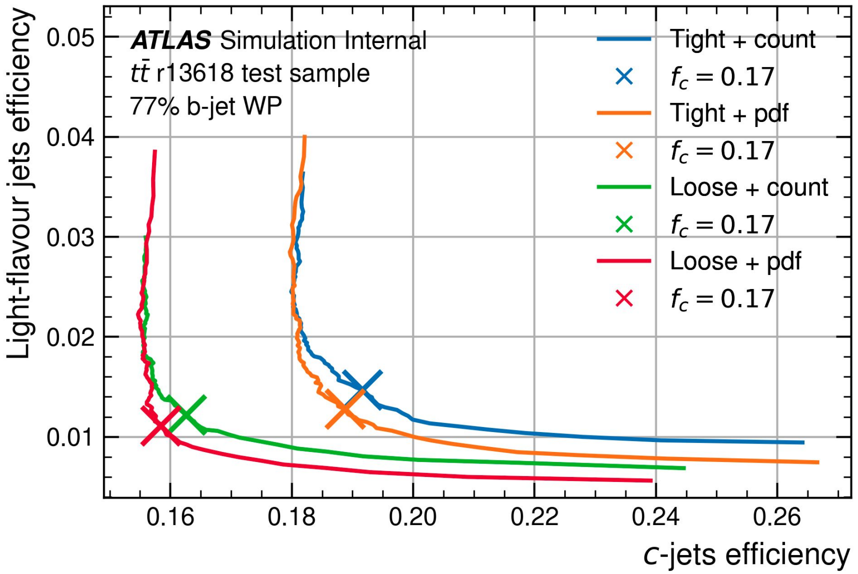

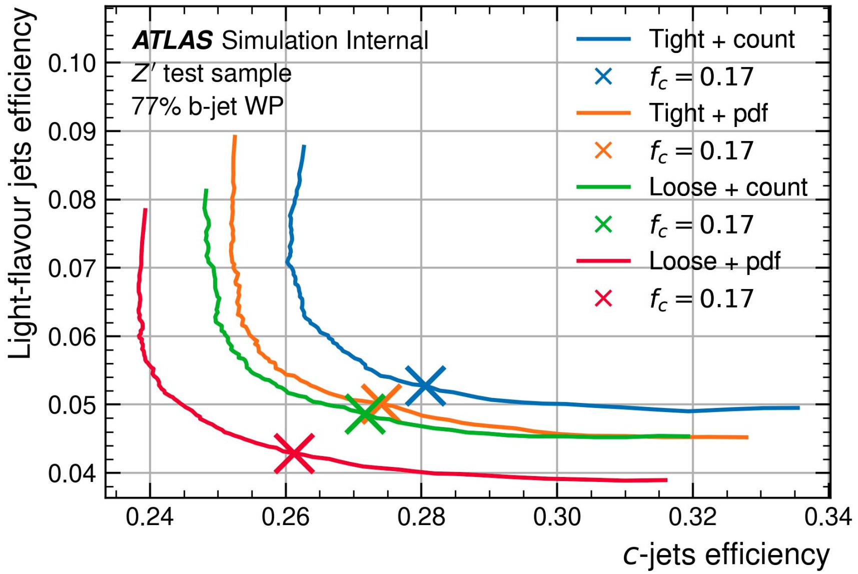

Graph neural network *b*-tagging algorithms

- GN1 inputs for upgrade training

Jet Input	Description
p_{T}	Jet transverse momentum
η	Signed jet pseudorapidity

Track Input	Description
q/p	Track charge divided by momentum (measure of curvature)
$\mathrm{d}\eta$	Pseudorapidity of the track, relative to the jet η
$\mathrm{d}\phi$	Azimuthal angle of the track, relative to the jet ϕ
d_0	Closest distance from the track to the PV in the longitudinal plane
$z_0 \sin\theta$	Closest distance from the track to the PV in the transverse plane
$\sigma(q/p)$	Uncertainty on q/p
$\sigma(\theta)$	Uncertainty on track polar angle θ
$\sigma(\phi)$	Uncertainty on track azimuthal angle ϕ
$s(d_0)$	Lifetime signed transverse IP significance
$s(z_0 \sin\theta)$	Lifetime signed longitudinal IP significance
nPixHits	Number of pixel hits
nStripHits	Number of strip hits
nInnermostPixHits	Number of hits from the innermost pixel layer
nNextToInnermostPixHits	Number of hits from the next-to-innermost pixel layer
nInnermostPixShared	Number of shared hits from the innermost pixel layer
nInnermostPixSplit	Number of split hits from the innermost pixel layer
nPixShared	Number of shared pixel hits
nPixSplit	Number of split pixel hits
nStripShared	Number of shared strip hits
nPixHoles	Number of pixel holes
nStripHoles	Number of strip holes

- Increase in performance allowed by GNNs for Run 2 and Run 3 [FTAG-2023-01]

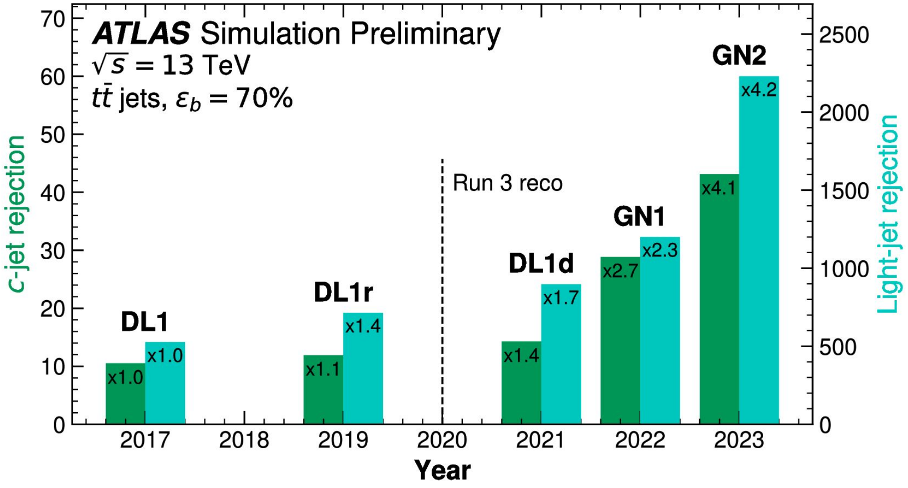

Signal selection efficiency

- Signal selection efficiency in the 1 *b*-tagged (left) and 2 *b*-tagged (right) jet regions

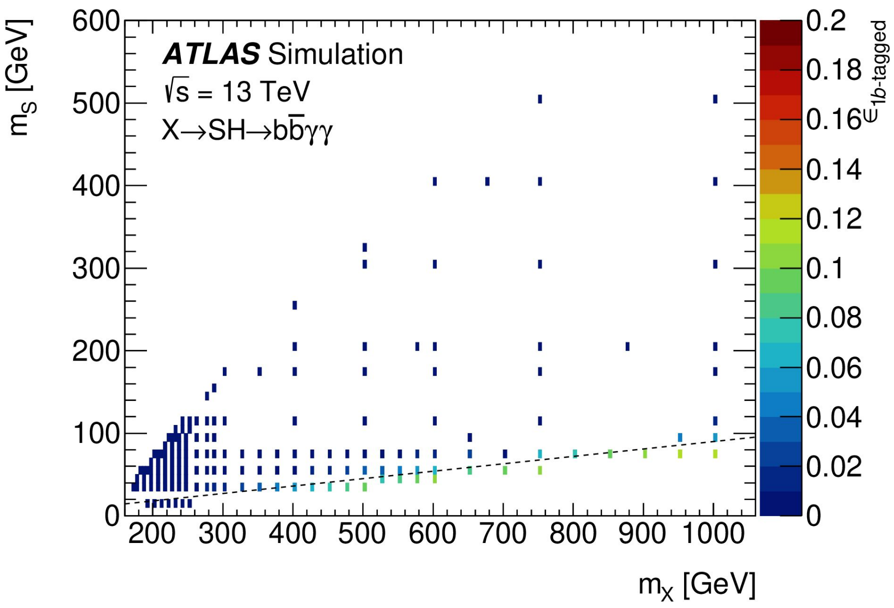

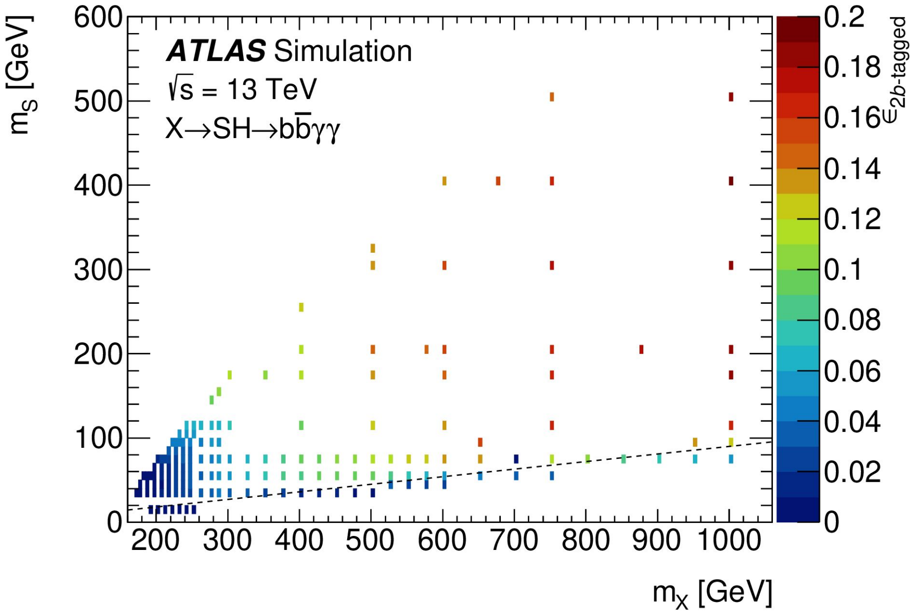

Expected number of events

- Obtained from a background only fit in the 2 *b*-tagged (left) and 1 *b*-tagged (right) jet regions

Background	2 b-tagged region Sideband	 Signal region	 Signal-like bin	1 b-tagged region Sideband	 Signal region	 Signal-like bin
Non-res. $\gamma\gamma$	1480 ± 37	372 ± 16	1.64 ± 0.37	13450 ± 110	3392 ± 53	2.45 ± 0.43
Single Higgs	0.46 ± 0.11	19.9 ± 5.3	0.04 ± 0.01	2.3 ± 1.1	92 ± 44	0.21 ± 0.10
ggF+$b\bar{b}H$	0.14 ± 0.11	6.5 ± 5.2	0.01 ± 0.01	1.5 ± 1.1	56 ± 43	0.11 ± 0.09
$t\bar{t}H$	0.21 ± 0.01	7.91 ± 0.77	0.01 ± 0.01	0.31 ± 0.01	11.4 ± 1.1	0.03 ± 0.01
ZH	0.08 ± 0.01	3.56 ± 0.30	0.02 ± 0.01	0.17 ± 0.01	7.35 ± 0.60	0.02 ± 0.01
Other	0.03 ± 0.01	1.94 ± 0.70	< 0.005	0.40 ± 0.23	17 ± 10	0.05 ± 0.03
Double Higgs	0.03 ± 0.01	1.65 ± 0.25	< 0.005	0.03 ± 0.01	1.79 ± 0.27	0.01 ± 0.01
Total	1480 ± 37	394 ± 16	1.67 ± 0.37	13450 ± 110	3486 ± 48	2.67 ± 0.45
Signal (m_X, m_S)						
(250, 100) GeV	0.38 ± 0.04	8.3 ± 1.2	1.43 ± 0.21			
(1000, 70) GeV				0.97 ± 0.10	33.3 ± 5.8	23.9 ± 4.2
Data	1479	395	0	13450	3491	4

PNN inputs

- 2 *b*-tagged region PNN inputs distribution

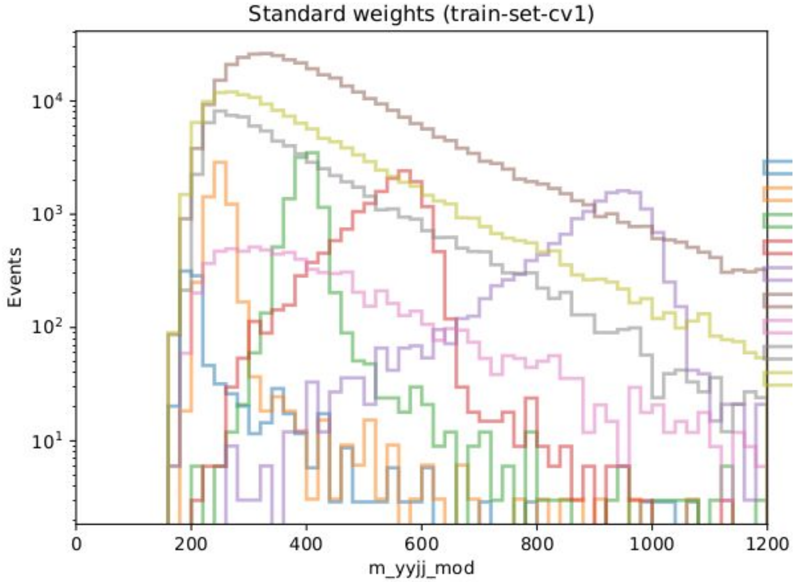

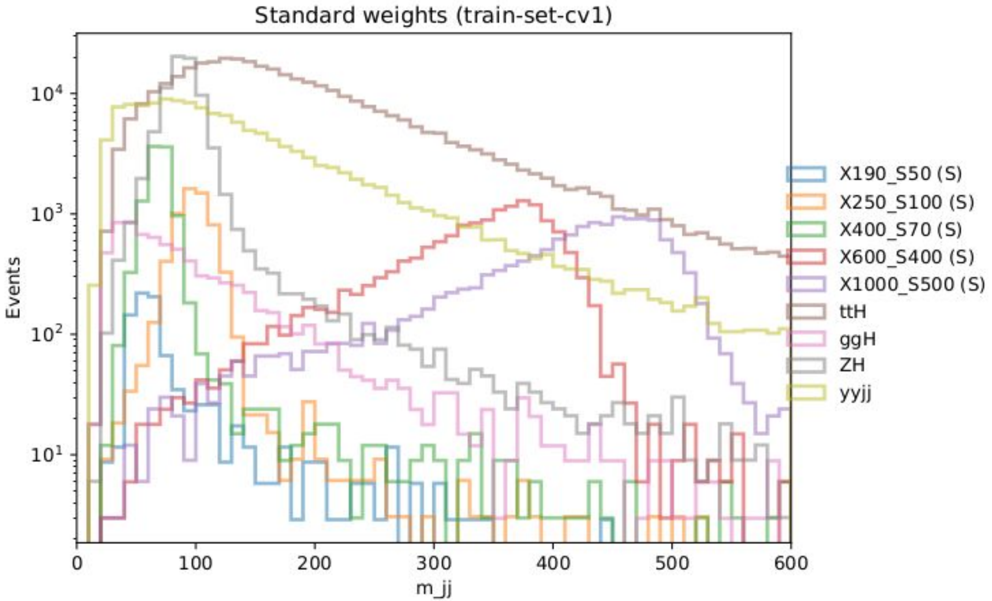

PNN inputs

- 1 *b*-tagged region PNN inputs distribution

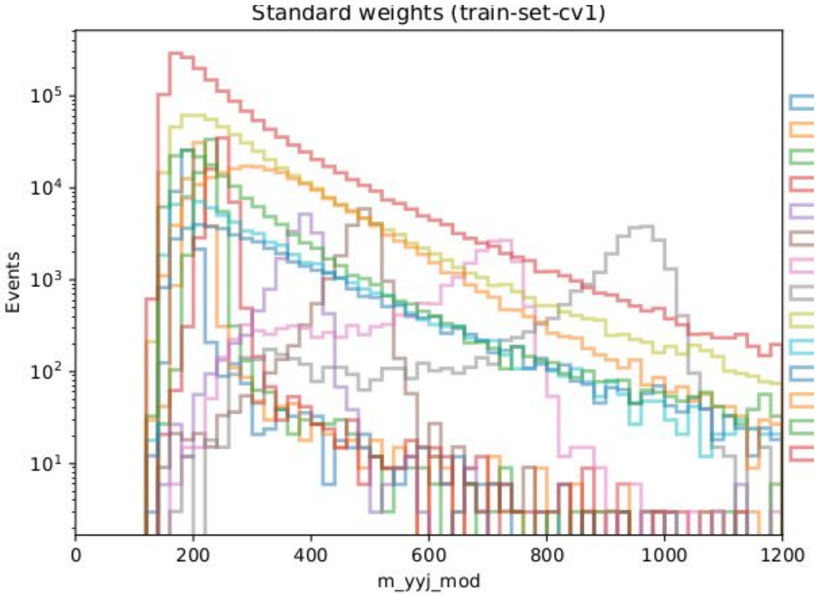

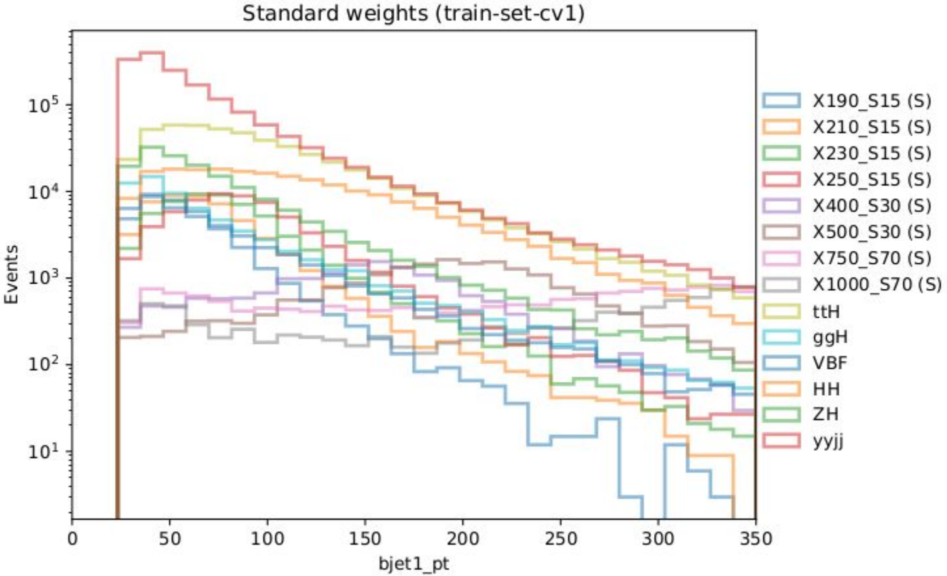

- Sensitivity comparison (expected limits) between the different analysis strategy

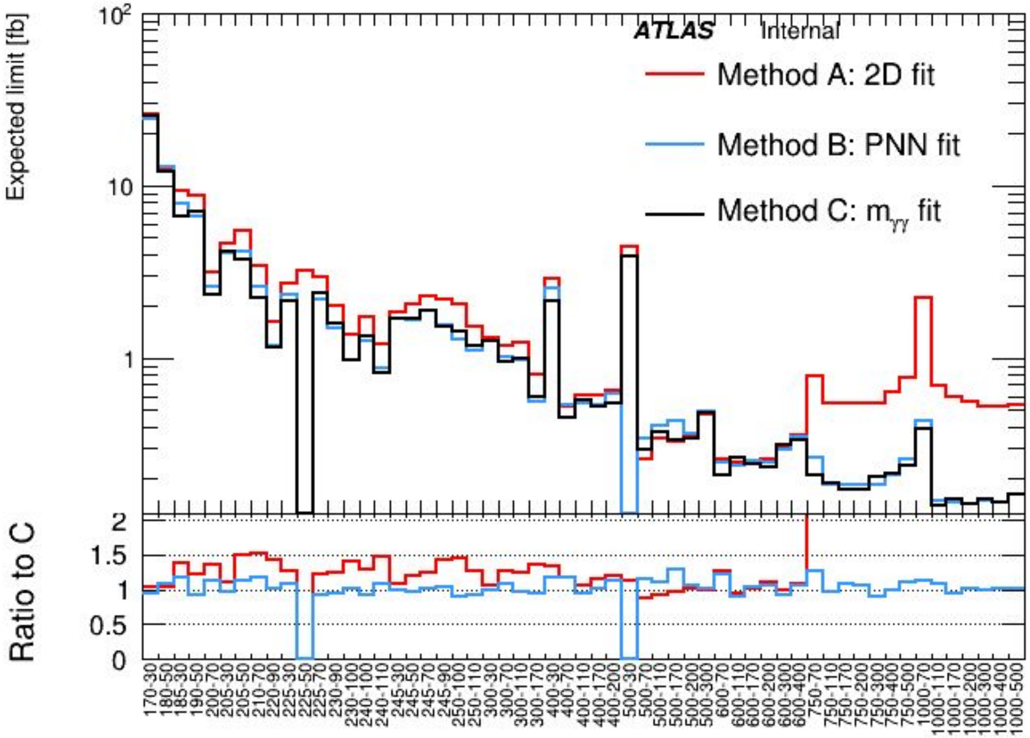

Data - MC agreement

- 2 *b*-tagged region PNN inputs sidebands distribution

$m_{bb\gamma\gamma}$*

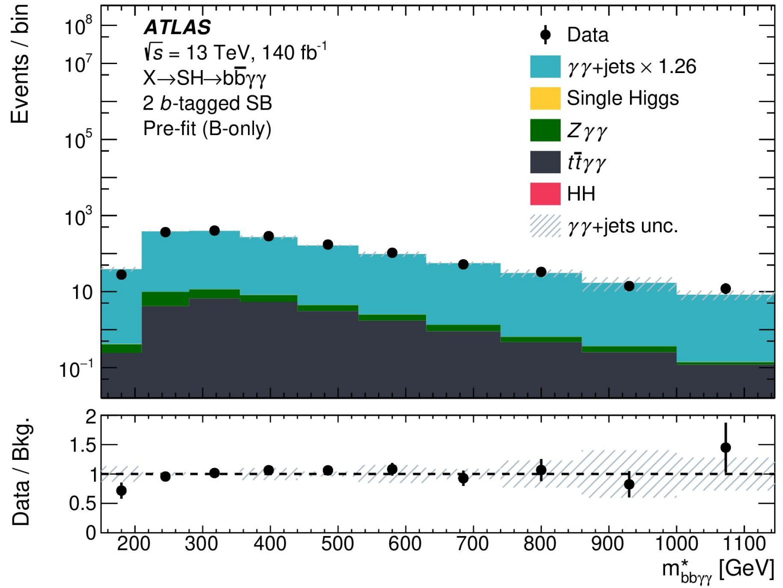

m_{bb}

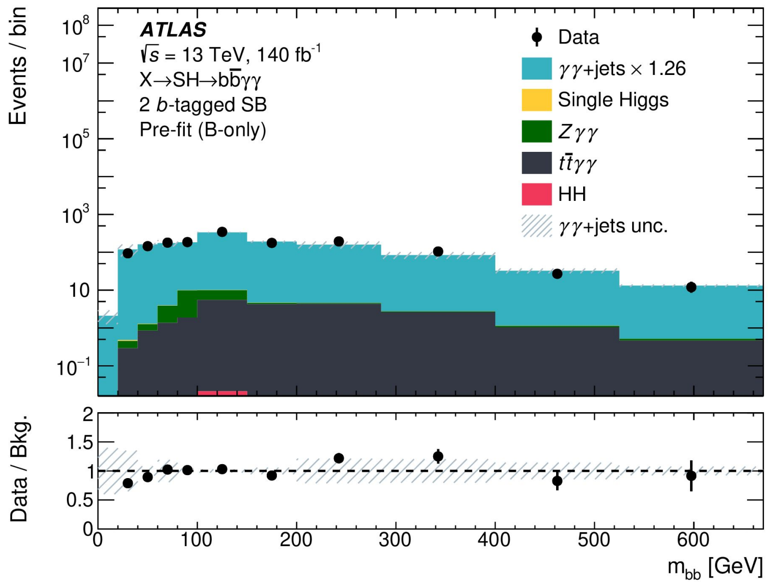

Data - MC agreement

- 1 *b*-tagged region PNN inputs sidebands distribution

$m_{b\gamma\gamma}{}^*$

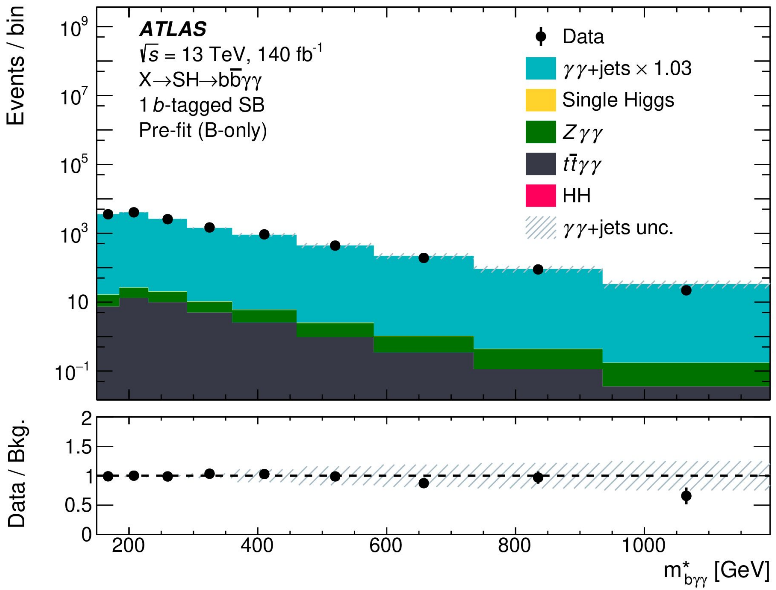

$p_T{}^b$

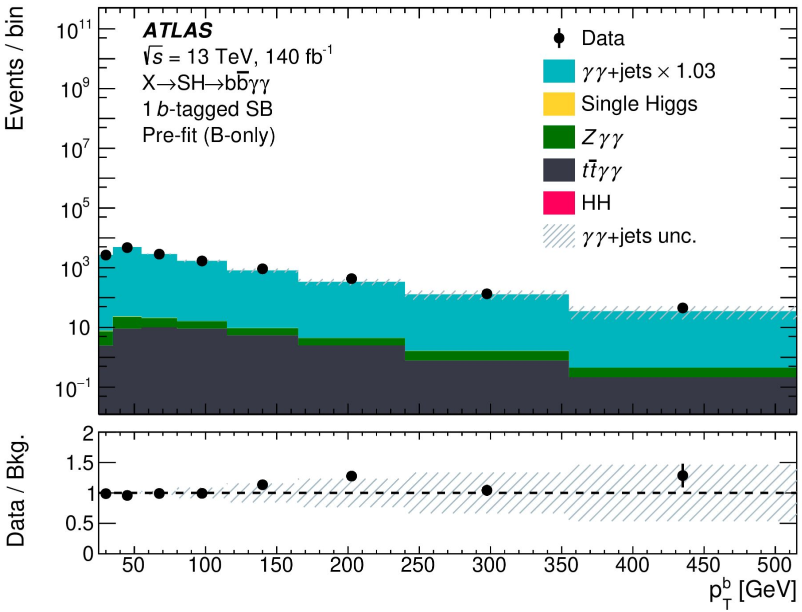

Systematic uncertainties

- Summary table of experimental and theoretical systematic uncertainties taken into account in the analysis

<table>
<tr><th colspan="2"></th><th>Signal</th><th>HH ggF</th><th>HH VBF</th><th>ttH & ZH</th><th>Other Single Higgs</th><th>Continuum $\gamma\gamma$+jets</th></tr>
<tr><td rowspan="2">Theory</td><td>Normalisation</td><td>$BR(H \to \gamma\gamma)$</td><td>$BR(H \to \gamma\gamma)$
$BR(H \to b\bar{b})$
PDF+α_S
Scales + m_t</td><td>$BR(H \to \gamma\gamma)$
$BR(H \to b\bar{b})$
PDF+α_S
Scales</td><td>$BR(H \to \gamma\gamma)$</td><td>$BR(H \to \gamma\gamma)$
PDF+α_S
Scales</td><td>$\gamma\gamma$
transfer
factor</td></tr>
<tr><td>Shape+Norm.</td><td>Scales, PDF+α_S
Parton shower
Interpolation</td><td>Parton Shower</td><td></td><td>Scales, PDF+α_S
Parton Shower</td><td></td><td>Scales, PDF+α_S
Modelling</td></tr>
<tr><td>Exp.</td><td>Shape+Norm.</td><td colspan="6">Pile-up modelling
Diphoton trigger efficiency
Photon identification and isolation efficiency
Photon energy scale and resolution (all exp. systematics are neglected for bbH, tH and VBF H)
Jet energy scale and resolution
Jet vertex tagger efficiency
Flavour tagging efficiency</td></tr>
</table>

Theoretical uncertainties impact

- Theoretical systematic uncertainties impact on the limit
  They are dominated by the γγ+jets modelling uncertainty

Impact at low m_X

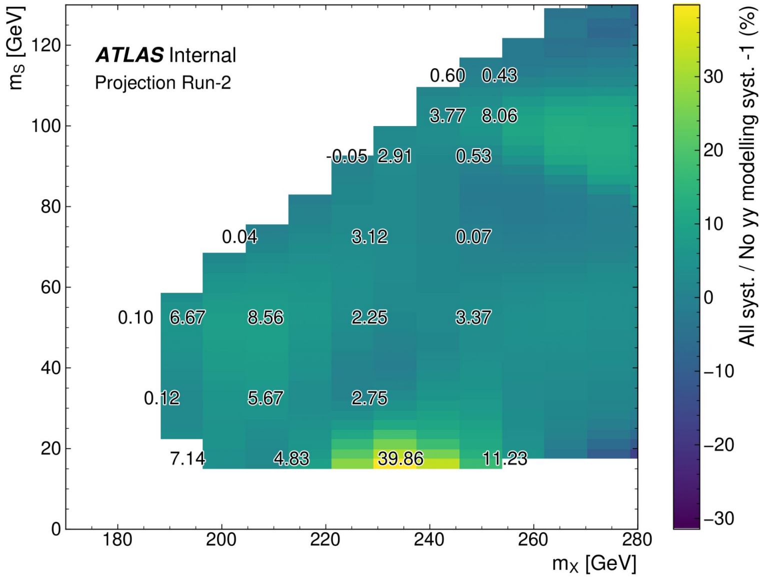

Impact at high m_X

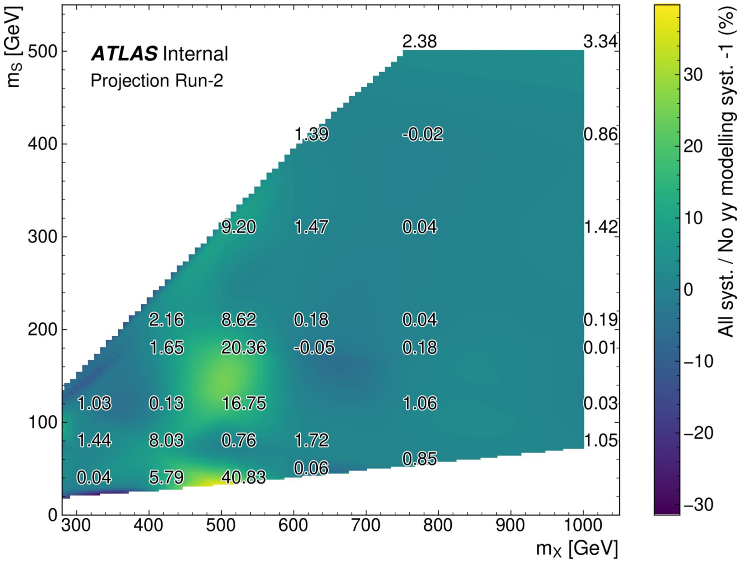

- The impact on the limit can be as large as 20% in the 2 *b*-tagged region and 40% in the 1 *b*-tagged region

Jet p_T

- Signal leading jet p_T distribution for two different mass points

(m_X, m_S) = (190, 50) GeV

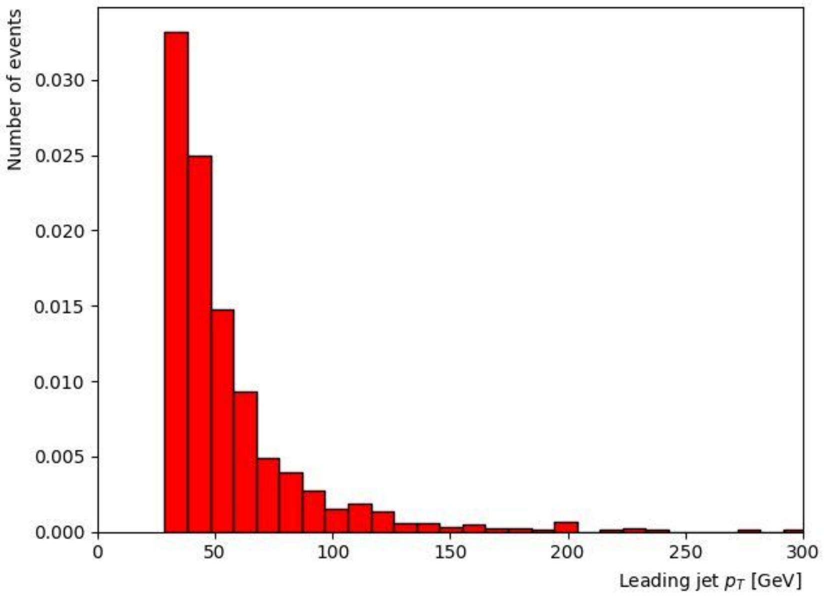

(m_X, m_S) = (750, 300) GeV

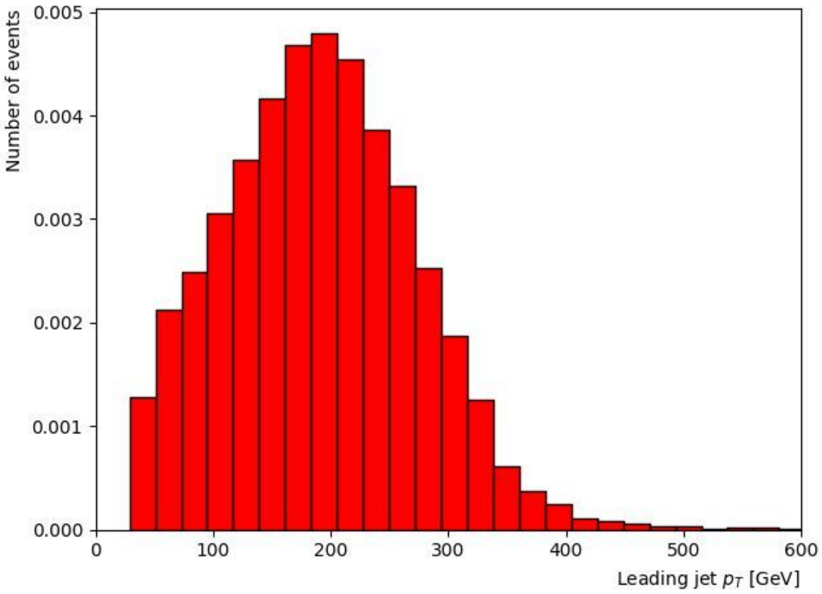

Ranking plots

- Example of ranking plots showing the impact on the fit of the 15 more important NP in two points

(m_X, m_S) = (250, 100) GeV - 2 *b*-tagged region

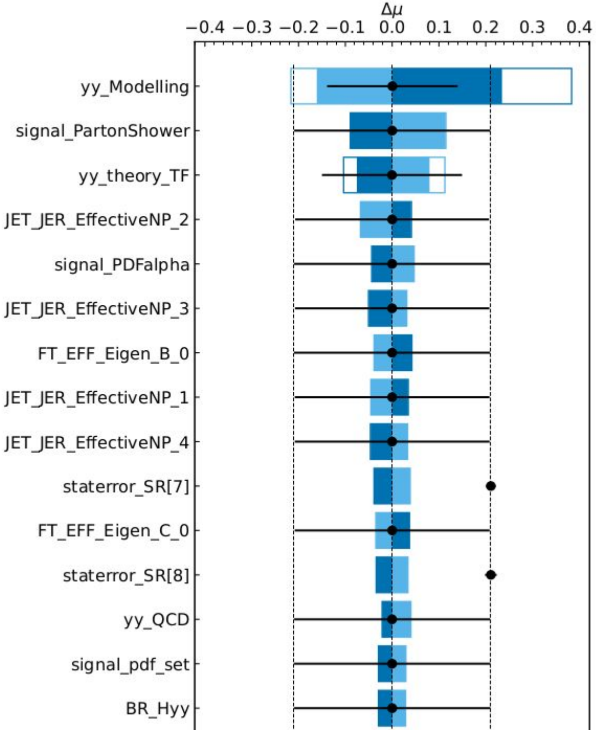

(m_X, m_S) = (230, 15) GeV - 1 *b*-tagged region

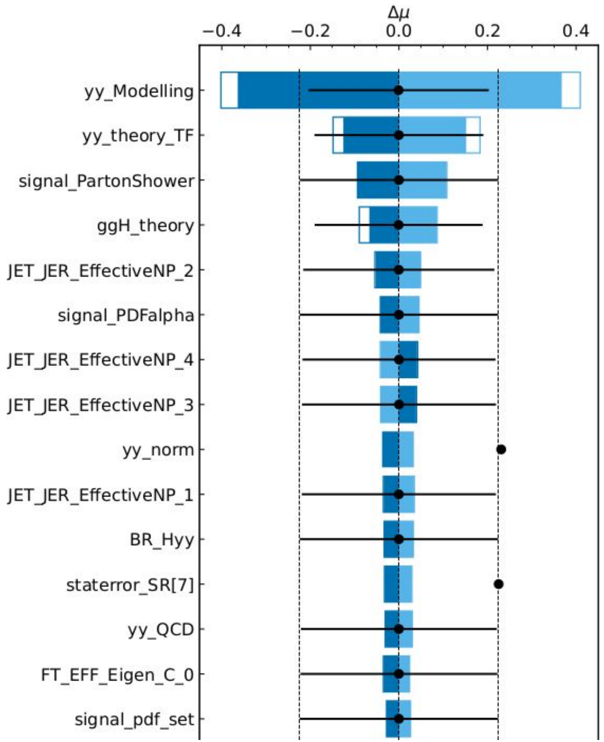

Interpolation

- Required granularity is assessed with signal injection tests to be sure not to miss any signal

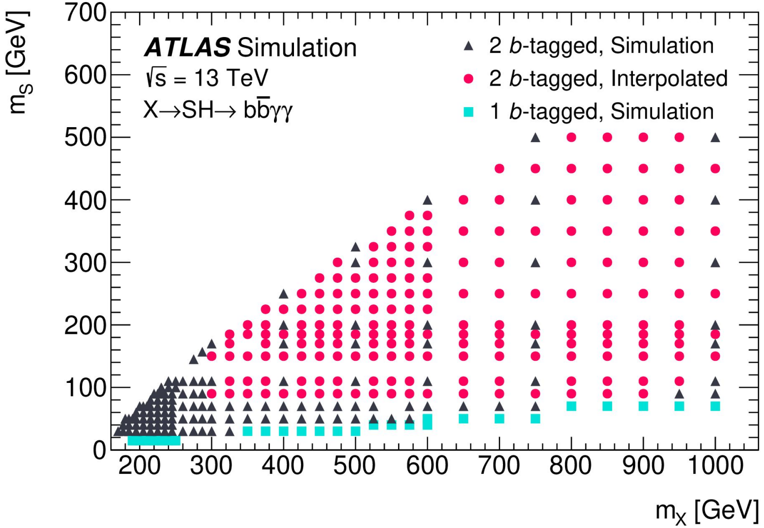

- For the red points, kinematic distributions are interpolated and used to compute PNN scores

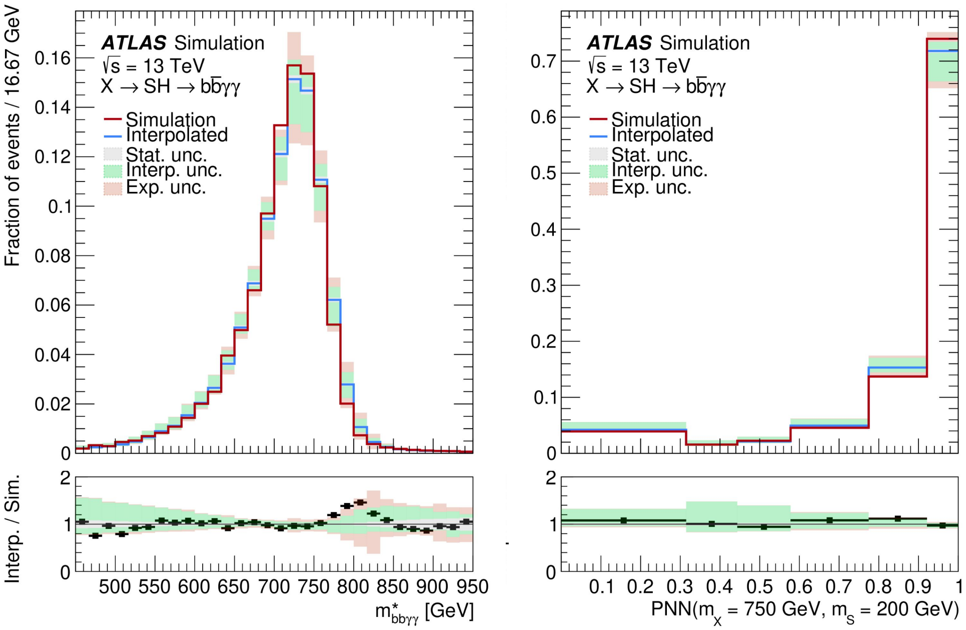

PNN and interpolation

- Example of PNN distribution in the 1 *b*-tagged region
  (m_X, m_S) = (1000, 70) GeV

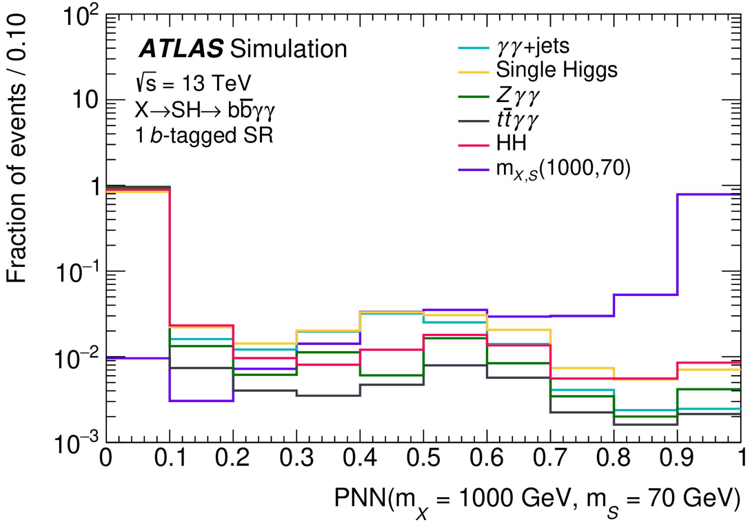

- PNNs are sensible to signals with masses close to their parameters

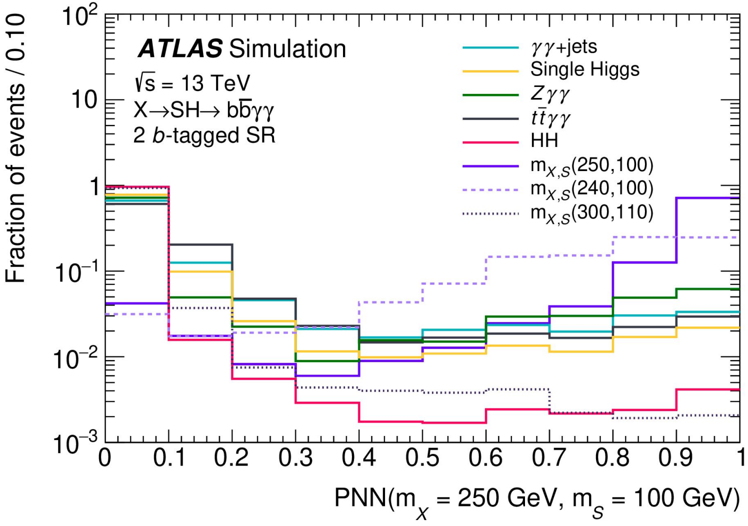

Post-fit PNN distributions

- SR post-fit PNN distribution for (m_X, m_S) = (250, 100) GeV (left - 2 *b*-tagged region) and (m_X, m_S) = (1000, 70) GeV (right - 1 *b*-tagged region)
  NB : signal distributions in blue normalised to σ = 1 fb

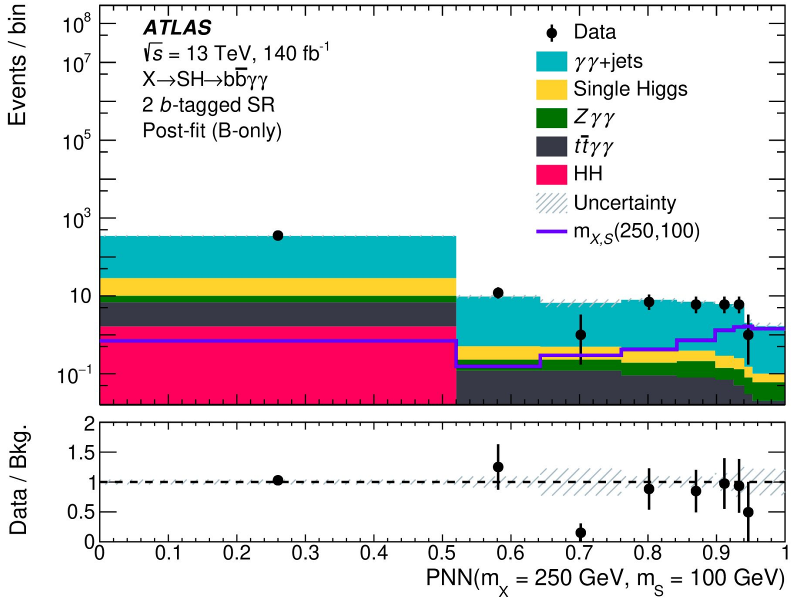

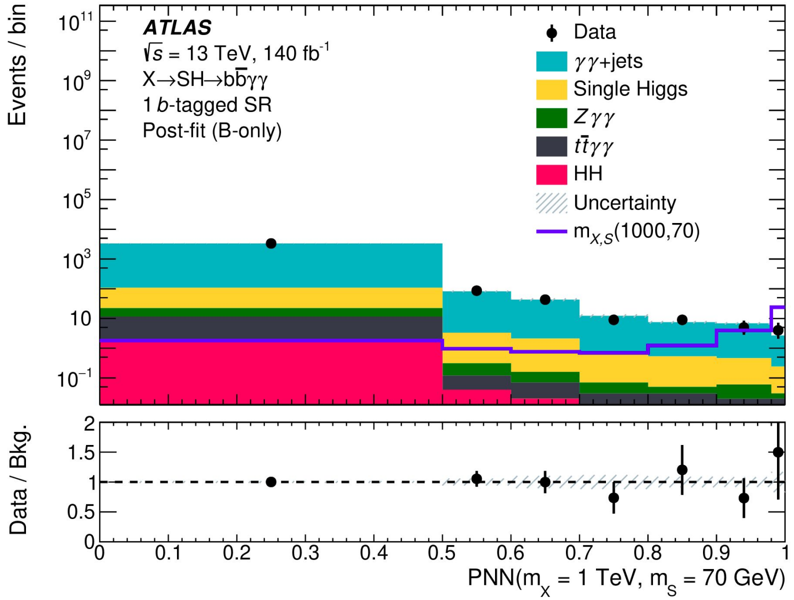

Expected limits

Low m_X

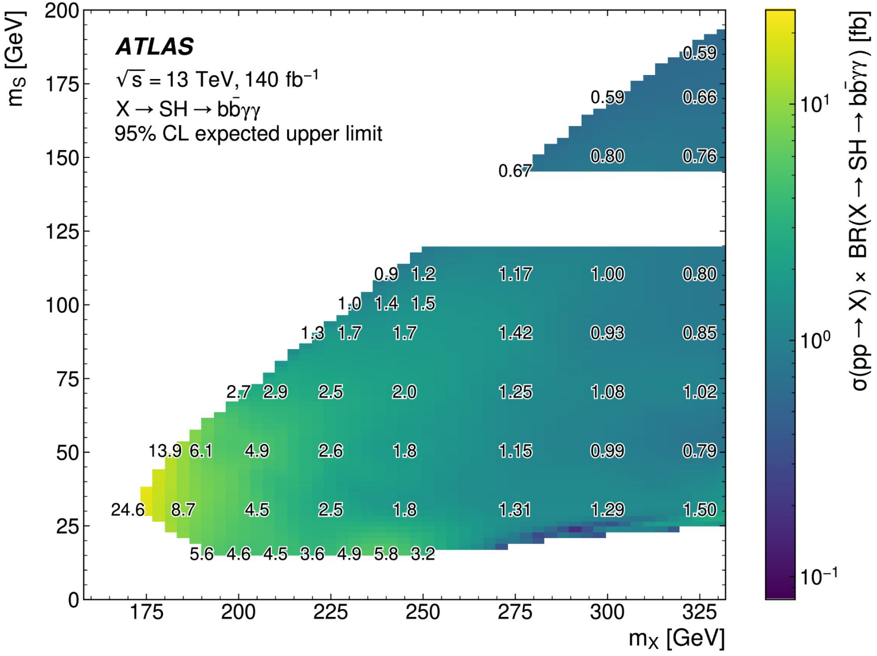

High m_X

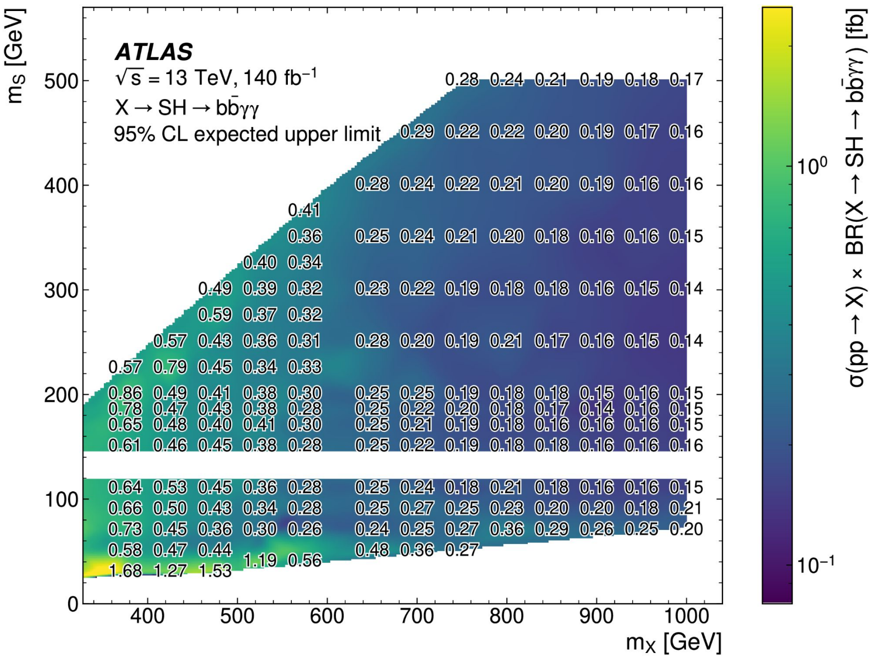

CMS $S/YH \to bb\gamma\gamma$ analysis

- JHEP 05 (2024) 316
- Mass range probed :
  $260 < m_X < 1000$ GeV, $90 < m_S$ / $m_Y < 800$ GeV

  → 6 different BDT in different (m_X, m_S) regions to discriminate signal from non resonant background
  → For $m_X < 550$ GeV DNN to discriminate signal from Resonant background

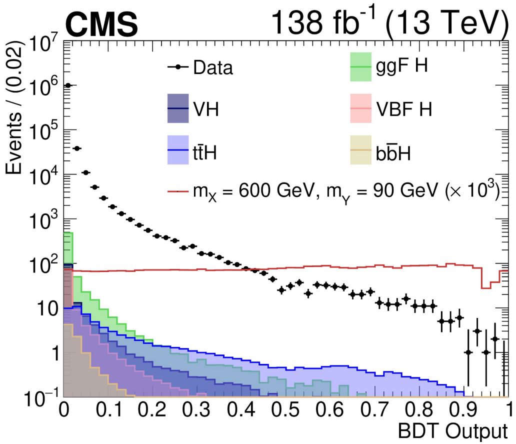

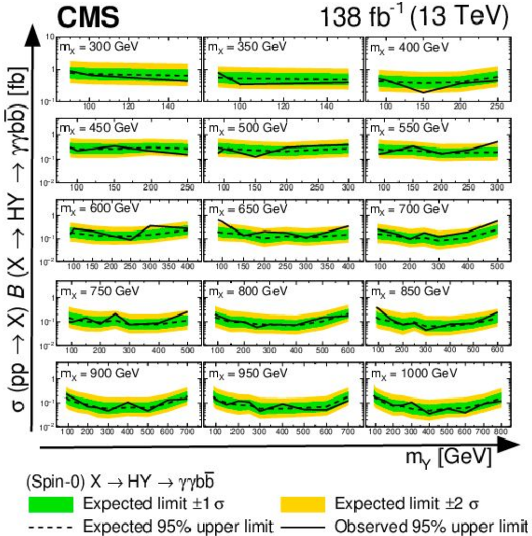

- Results obtained with a max. likelihood fit of the
  $m_{\gamma\gamma}$ and m_{jj} distributions

  Limits from 0.04 to 0.90 fb

CMS results - 3.8σ local excess

- Logal (global) 3.8σ (below 2.8σ) excess at (m_X, m_S) = (650, 90) GeV

- We perform a signal injection at the same point with a signal cross section of 0.35 fb (CMS best fit value)

  This signal injection gives an expected local excess of 2.7 standard deviation whereas we do not see any excess with respect to the background only hypothesis (p_0 > 0.5)

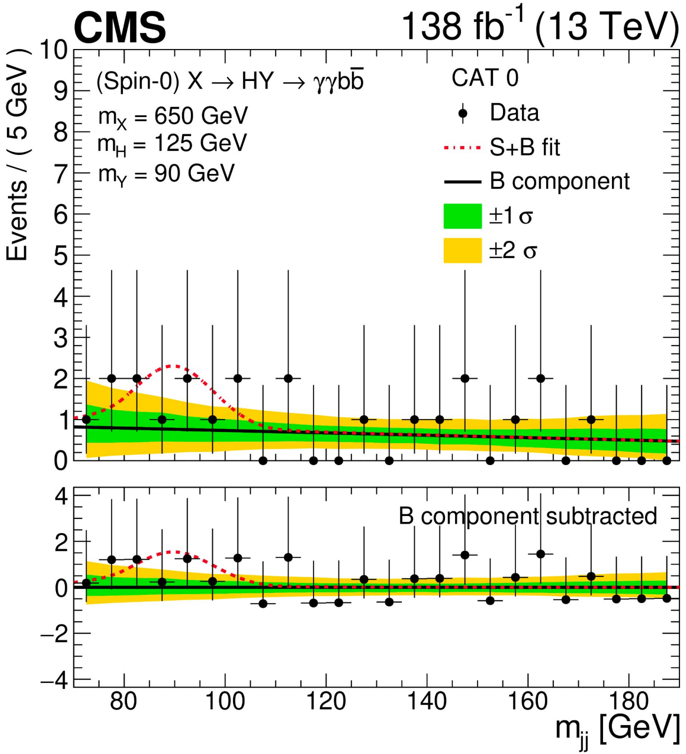

Other $X \to SH$ results in different channels

- CMS combination of *bbγγ*, *bbττ* and *4b* channels [arXiv:2403.16926]

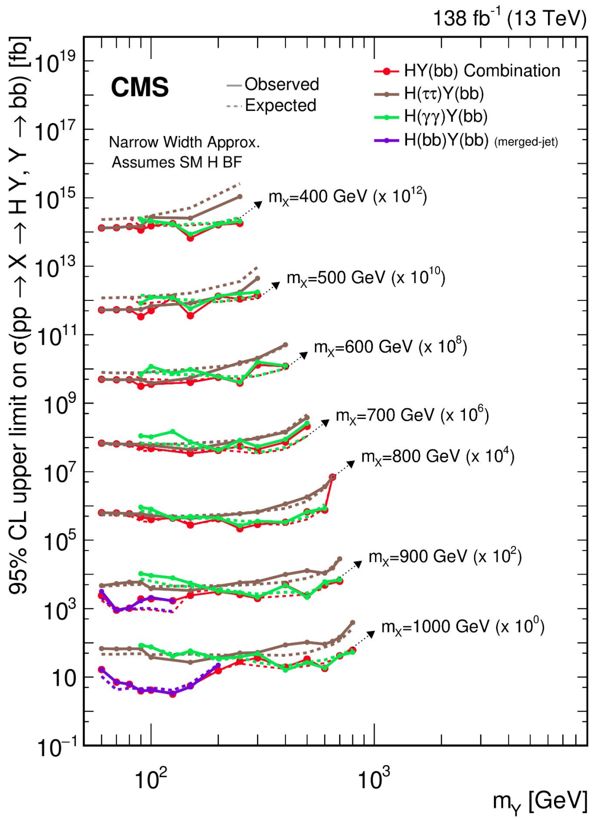

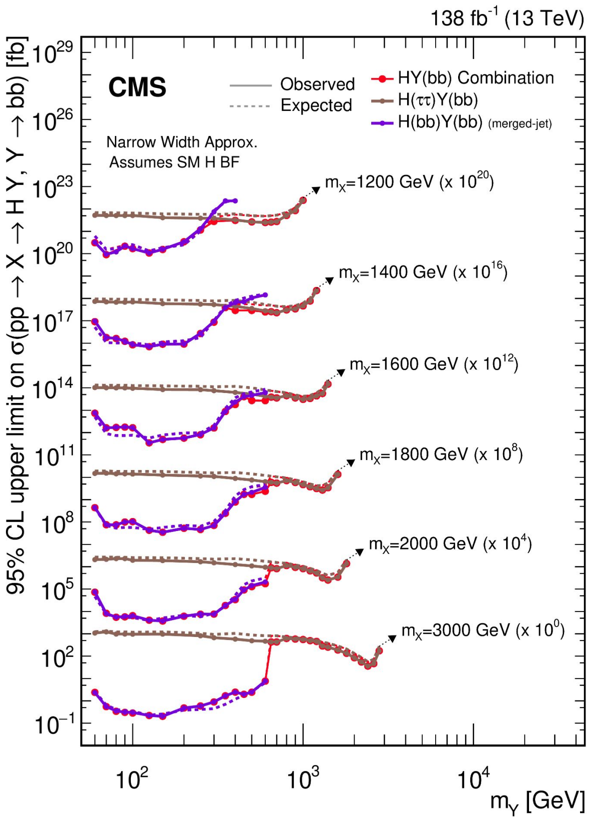

Non resonant *HH* analysis

- Resonant + non resonant *HH* → *bbγγ* paper [Phys. Rev. D 106 (2022) 052001]
  Legacy non resonant *HH* → *bbγγ paper* [JHEP 01 (2024) 066]